Received: 17 July 2019 | Revised: 7 October 2019 | Accepted: 8 October 2019

DOI: 10.1002/wnan.1602

ADVANCED REVIEW

WIREs NANOMEDICINE AND NANOBIOTECHNOLOGY WILEY

Protein-protected metal nanoclusters: An emerging ultra-small nanozyme

Xiangqin Meng[1,2] | **Iman Zare**[3] | **Xiyun Yan**[1,2,4] | **Kelong Fan**[2]

[1]School of Future Technology, University of Chinese Academy of Sciences, Beijing, China

[2]CAS Engineering Laboratory for Nanozyme, Key Laboratory of Protein and Peptide Pharmaceutical, Institute of Biophysics, Chinese Academy of Sciences, Beijing, China

[3]Department of Biology, Faculty of Basic Sciences, Semnan University, Semnan, Iran

[4]Joint Laboratory of Nanozymes in Zhengzhou University, Academy of Medical Sciences, Zhengzhou University, Zhengzhou, China

Correspondence
Xiyun Yan and Kelong Fan, CAS Engineering Laboratory for Nanozyme, Key Laboratory of Protein and Peptide Pharmaceutical, Institute of Biophysics, Chinese Academy of Sciences, Beijing, China.
Email: yanxy@ibp.ac.cn (X. Y.) and fankelong@ibp.ac.cn (K. F.)

Funding information
Chinese Academy of Sciences, Grant/Award Numbers: QYZDY-SSW-SMC013, XDPB29040101, YJKYYQ20180048; Ministry of Science and Technology of the People's Republic of China, Grant/Award Number: 2017YFA0205501; National Natural Science Foundation of China, Grant/Award Numbers: 31530026, 31871005, 31900981; Youth Innovation Promotion Association of the Chinese Academy of Sciences, Grant/Award Number: 2019093

Abstract

Protein-protected metal nanoclusters (MNCs), typically consisting of several to a hundred metal atoms with a protein outer layer used for protecting clusters from aggregation, are excellent fluorescent labels for biomedical applications due to their extraordinary photoluminescence, facile synthesis and good biocompatibility. Interestingly, many protein-protected MNCs have also been reported to exhibit intrinsic enzyme-like activities, namely peroxidase, oxidase and catalase activities, and are consequently used for biological analysis and environmental treatment. These findings have extended the horizon of protein-protected MNCs' properties as well as their application in various fields. Furthermore, in the field of nanozymes, protein-protected MNCs have emerged as an outstanding new addition. Due to their ultra-small size (<2 nm), they usually have higher catalytic activity, more suitable size for in vivo application, better biocompatibility and photoluminescence in comparison with large size nanozymes. In this review, we will systematically introduce the significant advances in this field and critically discuss the challenges that lie ahead. Ultra-small nanozymes based on protein-protected MNCs are on the verge of attracting great interest across various disciplines and will stimulate research in the fields of nanotechnology and biology.

This article is characterized under:
Therapeutic Approaches and Drug Discovery > Emerging Technologies
Biology-Inspired Nanomaterials > Protein and Virus-Based Structures

KEYWORDS
enzyme-like activities, metal nanoclusters, nanozymes, protein-protected metal nanoclusters, ultra-small nanomaterials

1 | INTRODUCTION

Metal nanoclusters (MNCs) (e.g., Au, Ag, Cu, Pt), made up of several to a hundred metal atoms, are a novel class of intermediates between metal atoms and nanoparticles (NPs). As their size (<2 nm) borders on the Fermi wavelength of electrons, the discrete energy levels lead MNCs to possess remarkably unique electrical, optical and chemical properties in comparison with large metal NPs (>2 nm) (Lu & Chen, 2012; Wilcoxon & Abrams, 2006). A characteristic feature is their strong

photoluminescence, combined with tuneable fluorescence emission, high photostability, large Stokes shift, good quantum yields and facile synthesis, making them excellent fluorescent labels for biomedical applications (Tao, Li, Ren, & Qu, 2015).

As for the synthesis of MNCs, the reduction of metal ions in liquid solution usually causes large NPs rather than small MNCs because MNCs tend to aggregate (P. Maity, Xie, Yamauchi, & Tsukuda, 2012). Therefore, suitable ligands capable of protecting clusters from aggregation are conventionally used for obtaining small, stable MNCs (Cui, Zhao, & Song, 2014). Up to now, various kinds of ligands such as glutathione, dendrimer, DNA and protein have been reported to assist the synthesis of MNCs (Jin, 2010; P. Maity et al., 2012). An emerging trend is using proteins as protective ligands (Figure 1a; Xavier et al., 2012). The functional groups (e.g., thiol, amino, carboxyl groups) in proteins have a strong affinity for noble metal atoms, making proteins become suitable ligands for binding and stabilizing MNCs (Shiang, Huang, Chen, Chen, & Chang, 2012). In 2009, bovine serum albumin (BSA) was first used to synthesize Au nanoclusters (NCs) by Xie et al. (Figure 1b; Xie et al., 2009). Following this work, other kinds of similar protein and self-designed peptide are also reported to act as efficient protective ligands for producing various MNCs. Compared with nonprotein ligands, proteins protected synthesis method has the following advantages: (a) it is a simple, effective, environmentally friendly synthetic route, usually reacting at physiological or indoor temperature in water without the addition of organic surfactants or hazardous regents, which possesses considerable environmental/cost advantages (W. T. Yang, Guo, Zhang, & Chang, 2014); (b) by regulating the structure and sequence of the protein, MNCs with different sizes and properties can be obtained (Dickerson, Sandhage, & Naik, 2008; Xavier et al., 2012); (c) the proteins can impart good biocompatibility and their own bioactivity to the resultant MNCs, and also facilitate postsynthesis surface modifications with functional ligands (Xie et al., 2009).

Due to the good biocompatibility and excellent photoluminescence, protein-protected MNCs as luminescent probes have received enormous attention and have been applied in a number of fields, such as biosensing, bioimaging, imaging-guided therapy, logic gate construction, temperature and pH meter (Chevrier, Chatt, & Zhang, 2012; Cui et al., 2014; C. G. Li, Chen, Chen, & Zhao, 2018; H. Li, Zhu, Wan, & Liu, 2017; Shang, Dong, & Nienhaus, 2011; Shiang et al., 2012; Y. Yu, Mok, Loh, & Tan, 2016). However, the enzyme-like property of protein-protected MNCs, a previously overlooked quality, is also starting to shine for basic research and practical application alike.

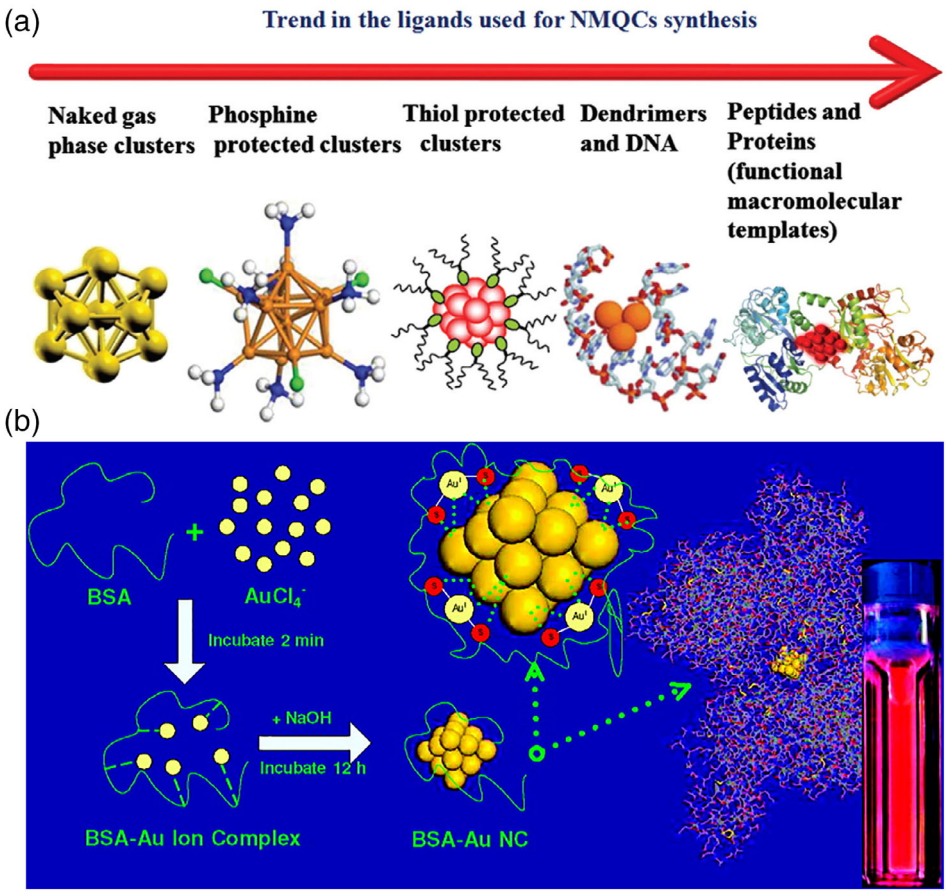

FIGURE 1 Protein as a protective ligand for the synthesis of MNCs. (a) Proteins are emerging as protective ligands for the synthesis of MNCs. (Reprinted with permission from Xavier, Chaudhari, Baksi, and Pradeep (2012). Copyright 2012 Taylor & Francis) (b) Schematic illustration of the formation of BSA-protected Au NCs. (Reprinted with permission from Xie, Zheng, and Ying (2009). Copyright 2009 American Chemical Society)

When it comes to nanomaterials and enzymatic activity, the term "nanozymes" (L. Gao & Yan, 2016)—nanomaterials with intrinsic enzyme-like activity—is often used. Since our group first discovered that Fe_3O_4 NPs, which are traditionally assumed as inert, possessed an intrinsic peroxidase-like activity (L. Z. Gao et al., 2007), substantial amount of work have focused on nanozymes due to their advantages, for example, high catalytic ability, high stability and low cost (L.-Z. Gao & Yan, 2013; Y. Huang, Ren, & Qu, 2019; Karakoti, Singh, Dowding, Seal, & Self, 2010; Meng & Fan, 2018; Wei & Wang, 2013; Wu et al., 2019). Nowadays, more than 540 kinds of nanomaterials including metal nanoparticle, metal oxide, metal sulfide and carbon based nanomaterials have been found to possess intrinsic enzymatic activities and have been used in biological analysis, environmental treatment, antibacteria, cancer therapy and antioxidation (Y. Huang et al., 2019; Ragg, Tahir, & Tremel, 2016). As ultra-small (<2 nm) nanomaterials, do protein-protected MNCs also have enzyme-like activity like large NPs (>2 nm)? Would protein-protected MNCs expand the type of nanozymes and become an emerging ultra-small one?

Recently, many efforts have been devoted to the exploration of enzyme mimetic activities of protein-protected MNCs and their potential applications. Up to now, the peroxidase, oxidase, and catalase enzymatic activities of protein-protected Au, Ag, Pt, Cu NCs have been discovered and subsequently been used for molecular diagnosis and pollutant removal (Table 1). In this review, we will systematically introduce these significant advances and discuss the future challenges in the construction of ultra-small protein-protected MNCs nanozymes for biomedical applications.

2 | PEROXIDASE NANOZYMES BASED ON PROTEIN-PROTECTED MNCS

Peroxidases are a class of enzymes that catalyze the reduction of hydrogen peroxide or lipid peroxide by a substrate which acts as an electron donor. Owing to their capacity to oxidize organic substances, for example, 3,3,5,5-tetramethylbenzidine (TMB) or 2,2 0-azino-bis(3-ethylbenzothiazoline-6-sulphonic acid) (ABTS) to colored product or enhance luminol chemiluminescence (CL), peroxidases have been widely applied in bioanalysis, clinical detection and environmental monitoring (Roda, Pasini, Mirasoli, Michelini, & Guardigli, 2004; Srisa-Art, Boehle, Geiss, & Henry, 2018). However, natural peroxidases have disadvantages such as high cost in preparation, low operational stability and short shelf life (Q. Y. Chen et al., 2000). Inspired by the first nanozyme—Fe_3O_4 peroxidase nanozyme, protein-protected MNCs which have facile synthesis and good colloidal stability have been paid more attention to explore their peroxidase catalytic activity and related applications as peroxidase mimics.

2.1 | Peroxidase nanozymes based on protein-protected Au NCs

In 2011, Wang's group first investigated the enzyme mimetic activity of protein-protected MNCs and discovered that BSA protected Au NCs exhibited peroxidase enzymatic activity (X. X. Wang et al., 2011). They synthesized Au NCs by reduction of Au ions with the tyrosine residues in BSA and then the Au NCs could be stabilized through a combination of Au—S bonding via the 35 Cysteine residues of BSA (Xie et al., 2009). Similar to peroxidase, the BSA-Au NCs can catalyze the oxidation of substrates, TMB and H_2O_2, to the oxidized colored product (Figure 2a). However, the BSA-Au NCs exhibited higher robustness and retained enzymatic activity over a wide range of pH and temperatures as compared to natural peroxidase. On the basis of H_2O_2 concentration dependence of the peroxidase activity of BSA-Au NCs, Wang's group developed a colorimetric sensor for the detection of H_2O_2. The results showed that H_2O_2 can be detected in the range from 5×10^{-7} to 2×10^{-5} M with a limit of detection (LOD) of 2×10^{-8} M. To detect xanthine, xanthine oxidase was used to produce H_2O_2 in the presence of xanthine, enabling further catalyzation by NCs. By combing the catalytic reaction of xanthine oxidase and BSA-Au NCs, xanthine can also be detected sensitively and selectively, even in urine and human serum samples. This work not only demonstrated the peroxidase enzymatic activity of BSA-Au NCs, but also exhibited potential applications of protein-protected MNCs nanozyme in analytical approaches in the future.

Although Wang's previous report proved the possibility of BSA-Au NCs as peroxidase mimics, their practical use has been limited because of the relatively low enzymatic activity and difficulty to separate and reuse (Cho et al., 2017). At this point, Kim et al. constructed nanohybrids by incorporating BSA-Au NCs and magnetic nanoparticles (MNPs; Cho et al., 2017). The nanohybrids yielded significantly enhanced peroxidase activity with five times higher affinity toward TMB than both BSA-Au NCs and MNPs due to synergistic catalytic enhancement. This may be attributed to the MNPs which have negative charge and attract the positively charged TMB onto the surface of nanohybrids more efficiently than the case with Au NCs only. Subsequently, they designed a highly sensitive glucose detecting method by combining the catalytic action of glucose oxidase and the nanohybrids (Figure 2b). The results demonstrated a linear range from 150 to 750 μM and a LOD of 100 μM.

TABLE 1 Representative examples of nanozymes based on protein-protected metal nanoclusters (MNCs) and their applications

Metal nanoclusters	Protective protein	Catalytic type	Catalytic activity	Application	Reference
Au NCs	BSA	Peroxidase	H_2O_2: $K_M = 25.3$ mM, $V_{max} = 7.21 \times 10^{-8}$ M/s, $K_{cat} = 9.17 \times 10^4$ s^{-1}; TMB: $K_M = 0.00253$ mM (125 times lower than that of HRP), $V_{max} = 6.23 \times 10^{-8}$ M/s, $K_{cat} = 7.24 \times 10^4$ s^{-1}	Colormetric detection of H_2O_2, LR: 5.0×10^{-7}–2.0×10^{-5} M, LOD: 2.0×10^{-8} M; of xanthine, LR: 1×10^{-6}–2×10^{-4} M, LOD: 5×10^{-7} M	X. X. Wang, Wu, Shan, and Huang (2011)
Graphene oxide-Au NCs	Lysozyme	Peroxidase	At pH 7.0, H_2O_2: $K_M = 142.39$ mM, $K_{cat} = 607.61$ s^{-1}; TMB: $K_M = 0.16$ mM (lower than that of HRP), $K_{cat} = 196.8$ s^{-1}; at pH 4.0, TMB: $K_{cat} = 236$ s^{-1}	Colormetric detection of MCF-7 cells, LOD: 1000 MCF-7 cells	Tao, Lin, Huang, Ren, and Qu (2013)
Au NCs	BSA	Peroxidase	The optimal pH is 4.0, the optimal temperature is 40°C; the catalytic activity can be inhibited by Hg^{2+}	Colormetric detection of Hg^{2+}, LR: 10nm–10 mM, LOD: 3 nM	Zhu et al. (2013)
Au NCs	BSA	Peroxidase	The catalytic activity greatly decreases due to the inhibition function of dopamine	Fluorometric and colorimetric detection of dopamine, LR: 10 nM–1 μM, LOD: 10 nM	Tao, Lin, Ren, and Qu (2013)
Au NCs	Human serum albumin (HSA)	Peroxidase	HSA-Au NCs can oxidize free bilirubin (with maximum absorbance at 440 nm) to mostly colorless compounds	Fluorometric and colorimetric detection of bilirubin, LOD: 0.25 and 0.20 μM, respectively	Santhosh, Chinnadayyala, Kakoti, and Goswami (2014)
Au NCs	BSA	Peroxidase	The optimal pH is 11.3 in sodium hydroxide solution	Luminol-based CL sensor for H_2O_2, LR: 2.0×10^{-8}–5.0×10^{-6} mol/L, LOD: 6×10^{-9} mol/L; for glucose, LR: 5.0×10^{-7}–1.0×10^{-5} mol/L, LOD: 1×10^{-7} mol/L	Deng, Xu, and Chen (2014)
Au NCs	BSA	Peroxidase	H_2O_2: $K_M = 2.46$ mM, $K_{cat} = 8.67 \times 10^4$ s^{-1} (significantly higher than that of HRP); TMB: $K_M = 0.00664$ mM (lower than that of HRP), $K_{cat} = 4.49 \times 10^4$ s^{-1} (significantly higher than that of HRP)	Tumor molecular colocalization diagnosis	D. Hu et al. (2014)
Au NCs	Apoferritin	Peroxidase	H_2O_2: $K_M = 199.4$ mM, $V_{max} = 9.34 \times 10^{-8}$ M/s, $K_{cat} = 7.2 \times 10^4$ s^{-1} (higher than that of HRP); TMB: $K_M = 0.097$ mM (four times lower than that of HRP), $V_{max} = 7.46 \times 10^{-8}$ M/s, $K_{cat} = 5.8 \times 10^4$ s^{-1} (higher than that of HRP); more stable than HRP, maintained the activity at different pH (0–12) and temperatures (4–70°C)	Colormetric detection of glucose, LR: 2.0–10.0 mM	Jiang, Sun, Guo, Nie, and Xu (2015)
Au NCs	BSA	Peroxidase	The optimal pH is 4.0; the catalytic activity can be inhibited by Cys and then restored by Hg^{2+}	Colormetric detection of Cys, LR: 0.2–60 μM, LOD: 80 nM; of Hg^{2+}, LR: 0.2–60 μM, LOD: 30 nM	Y.-W. Wang, Tang, Yang, and Song (2016)
Au NCs	BSA	Peroxidase			

(Continues)

TABLE 1 (Continued)

Metal nanoclusters	Protective protein	Catalytic type	Catalytic activity	Application	Reference
			The optimal pH is 4.0, the optimal temperature is 25–35°C; the catalytic activity can be inhibited by Ag^+	Colormetric detection of Ag^+, LR: 0.5–10 μM, LOD: 0.204 μM	Chang, Zhang, Hao, Yang, and Tang (2016)
Fe_3O_4-Au NCs	BSA	Peroxidase	H_2O_2: $K_M = 79$ mM (lower than that of Fe_3O_4 or Au NCs), $V_{max} = 4.6 \times 10^{-5}$ M/s; TMB: $K_M = 0.24$ mM (about 20% of the value of Fe_3O_4 or Au NCs), $V_{max} = 9.6 \times 10^{-7}$ M/s	Colormetric detection of H_2O_2, LR: 150–5,000 μM, LOD: 100 μM; of glucose, LR: 150–750 μM, LOD: 100 μM	Cho, Shin, and Kim (2017)
Au NCs	Protamine	Peroxidase	H_2O_2: $K_M = 1.49$ mM (2.5 times lower than that of HRP), $V_{max} = 2.8 \times 10^{-6}$ M/s; TMB: $K_M = 0.169$ mM (much lower than that of HRP), $V_{max} = 1.84 \times 10^{-6}$ M/s; the catalytic activity can be improved by Hg^{2+}	Colormetric detection of Hg^{2+}, LR: 4.0 nM–1.0 μM, LOD: 1.16 nM	Y. Q. Huang et al. (2018)
Cationic Au NCs	BSA	Peroxidase	At pH 5, and catalytic activity of cationic Au NCs was about twofold higher than that of Au NCs; at pH 6 and pH 7, an obvious peroxidase activity of cationic Au NCs was observed while Au NCs has no enzymatic activity		Han, Li, and Fan (2018)
Mesoporous silica nanoparticles (MSN)-Au NCs	Lysozyme	Peroxidase	The catalytic ability of MSN-Au NCs-anti-HER2 relied on MSN-Au NCs-anti-HER2 concentration, H_2O_2 concentration, temperature and pH	Colormetric detection of HER2+ breast cancer cell, LR: 10–1,000 cells, LOD: 10 cells; this method can also measure breast cancer tissues with different HER2 expression levels	M. Q. Li et al. (2019)
Au NCs	Peptide substrates of serine protease thrombin and the zinc-dependent matrix metalloproteinase 9	Peroxidase	TMB: $K_M = 0.23$ mM (lower than that of HRP), $V_{max} = 3.6 \times 10^{-7}$ M/s, $K_{cat} = 0.2$ s^{-1}; retain catalytic activity after filtered through the kidneys and into urine	In vivo cancer monitoring, catalytic activity of Au NCs in the urine of tumor-bearing mice showed 13-fold increase than that of healthy mice	Loynachan et al. (2019)
Pt NCs	Ferritin	Peroxidase	The optimal pH is 4, the optimal temperature is 25°C; H_2O_2: $K_M = 187.25$ mM, $V_{max} = 3.2 \times 10^{-4}$ M/s; TMB: $K_M = 0.22$ mM (13-fold lower than that of HRP), $V_{max} = 5.58 \times 10^{-7}$ M/s		J. Fan et al. (2011)
Pt NCs	BSA	Peroxidase	H_2O_2: $K_M = 41.8$ mM, $V_{max} = 1.67 \times 10^{-7}$ M/s (faster than that of HRP); TMB: $K_M = 0.119$ mM (three times lower than that of HRP),	Colormetric detection of Hg^{2+}, LR: 0–120 nM, LOD: 7.2 nM	W. Li et al. (2015)

(Continues)

TABLE 1 (Continued)

Metal nanoclusters	Protective protein	Catalytic type	Catalytic activity	Application	Reference
			$V_{max} = 2.1 \times 10^{-7}$ M/s (faster than that of HRP); the catalytic activity can be downregulated by Hg^{2+}		
Cu NCs	BSA	Peroxidase	H_2O_2: $K_M = 29.16$ mM, $V_{max} = 4.22 \times 10^{-8}$ M/s; TMB: $K_M = 0.648$ mM, $V_{max} = 5.96 \times 10^{-8}$ M/s	Colormetric detection of H_2O_2, LR: 10 μM–1 mM, LOD: 10 μM; of glucose, LR: 100 μM–2 mM, LOD: 100 μM	L. Hu et al. (2013)
Cu NCs	BSA	Peroxidase	The optimal pH is 11.8, some organic compounds containing OH, NH_2, or SH groups can inhibit the catalysis of Cu NCs	Luminol-based CL sensor for H_2O_2, LR: 0.1–150 mM, LOD: 0.03 mM	Xu, Chen, Deng, and Sui (2014)
Cu NCs	BSA	Peroxidase	The optimal pH is 12	Luminol-based CL sensor for cholesterol, LR: 0.05–10 mM, LOD: 1.5 μM	Xu et al. (2016)
Cu NCs	BSA	Peroxidase	H_2O_2: $K_M = 8.9 \times 10^{-3}$ mM, $V_{max} = 8.42 \times 10^{-6}$ M/s; TMB: $K_M = 1.38 \times 10^{-3}$ mM (17 times lower than that of HRP), $V_{max} = 2.33 \times 10^{-5}$ M/s; the optimal reaction condition was pH 3.5 and 50°C	Colormetric detection of xanthine, LR: 5.0×10^{-7}–1.0×10^{-4} mol/L, LOD: 3.8×10^{-7} mol/L	Yan et al. (2017)
Cu NCs	BSA	Peroxidase	In the presence of H_2O_2, BSA-Cu NCs can fasten the oxidation of dopamine to dopaquinone which acts as a fluorescence quencher	Fluorescence-based detection of dopamine, in the presence of H_2O_2, LOD: 0.1637 pM; in the absence of H_2O_2, LOD: 0.024 nM	Aparna, Devi, Nebu, Syamchand, and George (2019)
Au NCs	BSA	Oxidase	Red BSA-Au NCs, TMB: $K_M = 0.08$ mM (much lower than that of HRP), $V_{max} = 9.57 \times 10^{-8}$ M/s; blue BSA-Au NCs, TMB: $K_M = 0.1$ mM (much lower than that of HRP), $V_{max} = 2.322 \times 10^{-7}$ M/s; the catalytic activity can be downregulated by trypsin	Colormetric detection of trypsin, LR: 0.9 μg/ml–1.0 mg/ml, LOD: 0.6 μg/ml	G. L. Wang, Jin, Dong, Wu, and Li et al. (2015)
Ag NCs	BSA	Oxidase		Colorimetric immunoassay for *Listeria monocytogenes*, LR: 10–10^6 cfu/ml, LOD: 10 cfu/ml	Liu et al. (2018)
Pt NCs	Lysozyme	Oxidase	TMB: $K_M = 0.63$ mM, $V_{max} = 2.7 \times 10^{-6}$ M/s, a lower K_M value and a higher V_{max} value than that of CeO_2 NPs	Degrade methylene blue in the absence of H_2O_2	C. J. Yu, Chen, Jiang, and Tseng (2014)
Pt NCs	Ferritin	Catalase	The optimal pH is 12, the optimal temperature is 85°C; H_2O_2: $K_M = 420.6$ mM, $V_{max} = 8.4 \times 10^{-4}$ M/s		J. Fan et al. (2011)

Abbreviations: LOD, limit of detection; LR, linear range.

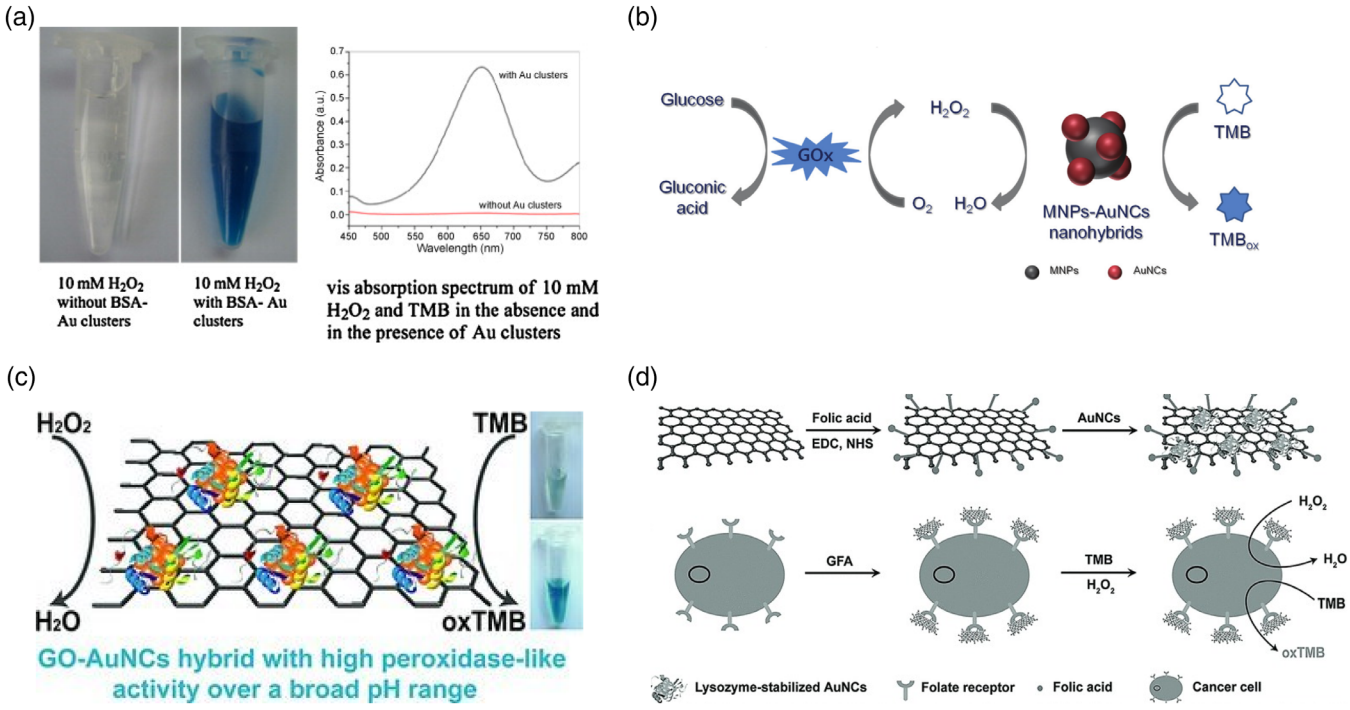

FIGURE 2 Protein-protected Au NCs as effective peroxidase nanozymes and the improvement of their catalytic activity. (a) BSA-protected Au NCs exhibit peroxidase enzymatic activity. (Reprinted with permission from X. X. Wang et al. (2011). Copyright 2011 Elsevier B.V.) (b) MNPs-Au NCs with enhanced peroxidase activity for the detection of glucose. (Reprinted with permission from Cho et al. (2017). Copyright 2017 AIP Publishing) (c) GO-Au NCs with high peroxidase enzymatic activity over a wide pH range. (d) The target-directed GO-lysozyme-Au NC hybrid used for cancer cell detection. (Reprinted with permission from Tao, Lin, Huang, et al. (2013). Copyright 2013 Wiley-VCH Verlag GmbH & Co. KGaA)

Despite these progresses, there remains one critical shortcoming in protein-protected MNCs. Due to the poor solubility of TMB in a base medium (He et al., 2011), the optimum pH of these enzyme mimics is usually near 3, which seriously limits its use in biological conditions with the pH between 5.0 and 7.4. In light of this, Qu et al. reported that graphene oxide (GO) can act as an enzyme modulator to regulate lysozyme-protected Au NCs' peroxidase enzymatic activity. Interestingly, the developed GO-lysozyme-Au NCs hybrid (GA) showed highly enzymatic activity over a wide pH range even including pH 7.4 (Figure 2c; Tao, Lin, Huang, et al., 2013). They further analyzed the catalytic mechanism of GA activity at neutral pH. The results showed that in the presence of GO which had high affinity for hydrophobic molecules and high surface-to-volume ratios, TMB was absorbed onto GO more efficiently. Then, the absorbed TMB and lysozyme-Au NCs on GO sheets were limited in a nanoscale region, which quite improved the enzymatic activity at neutral pH (Dong et al., 2012). Taking advantage of the high peroxidase activity of GA at neutral pH, they developed a folic acid conjugated GO-lysozyme-Au NC hybrid as a nanozyme nanoprobe for rapid colorimetric detection of cancer cells (Figure 2d). This work may facilitate the utilization of peroxidase nanozymes based on protein-protected MNCs for numerous feasible applications in biological conditions in which a neutral pH is required.

CL has become an important and useful tool in many fields, for example, environmental analysis, bioanalysis and clinical detection because of its advantages of extremely high sensitivity and simple instrumentation (Ahmed et al., 2009; Xiao et al., 2009; Yamasuji, Shibata, Kabashima, & Kai, 2011). Luminol, commonly used in CL reactions, is another major substrate of peroxidase (Kricka, 1995). Chen's group first explored the enzymatic property of BSA-Au NCs in luminol CL systems, and discovered that BSA-Au NCs can boost CL spectra of the luminol-hydrogen peroxide system like a peroxidase (Figure 3a; Deng et al., 2014). However, its catalytic activity was still lower than that of natural horseradish peroxidase (HRP) for the use in CL reactions (Han et al., 2018). Following this work, Fan et al. investigated whether the surface charge of NCs could regulate the enzymatic property of BSA-Au NCs (Han et al., 2018). Interestingly, cationic BSA-Au NCs showed much higher enzymatic activity in the luminol–H_2O_2 CL system than that of unmodified Au NCs (Figure 3b). They proved that cationic Au NCs may profit by the interaction of •OH and $O_2^{\bullet-}$ to give rise to $^1O_2$ which is responsible for the oxidation of luminol. Additionally, the O_2 around cationic Au NCs may also help generate $^1O_2$. Moreover, the positive charge of the cationic Au

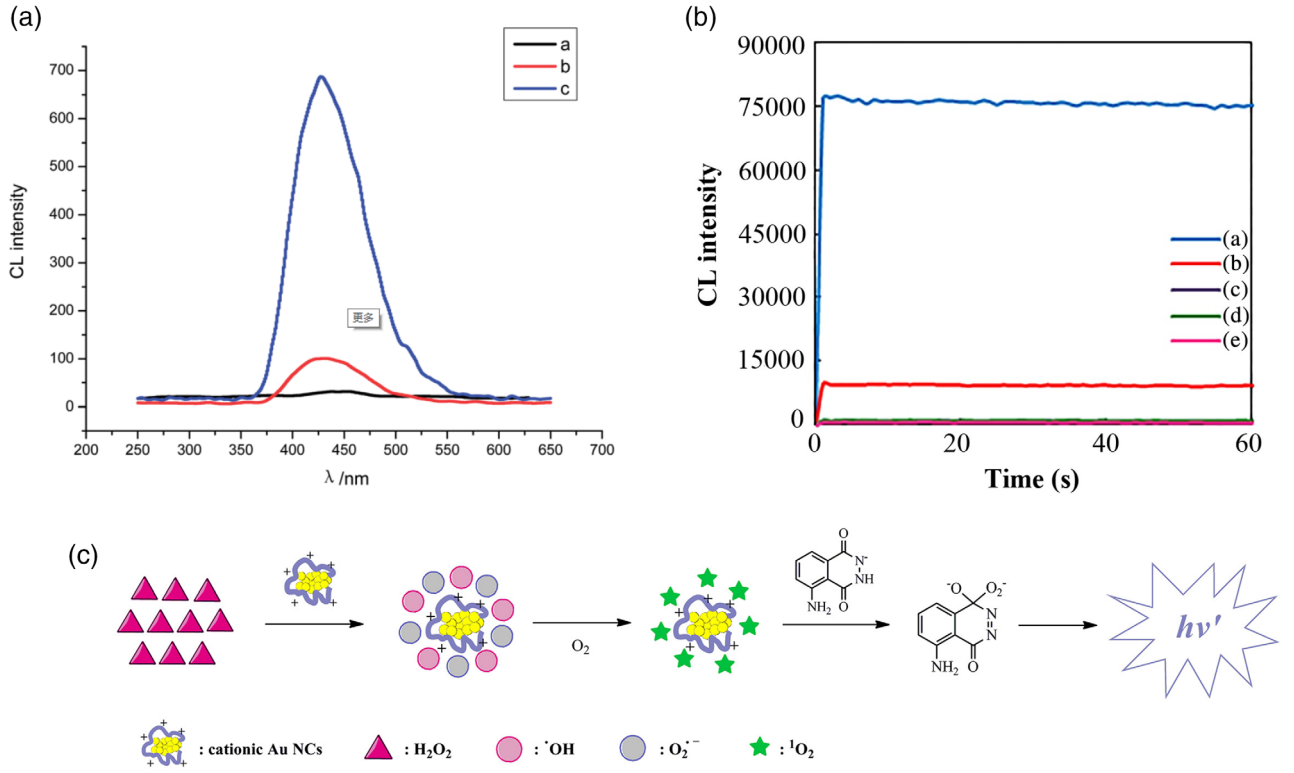

FIGURE 3 Protein-protected Au NCs as effective peroxidase nanozymes enhance CL of the luminol–H_2O_2 system. (a) CL kinetic curves of the luminol–H_2O_2–Au NCs system: (a) Au NCs; (b) luminol–H_2O_2; (c) luminol–H_2O_2–Au NCs. (Reprinted with permission from Deng et al. (2014). Copyright 2014 The Royal Society of Chemistry) (b) CL spectra of the luminol–H_2O_2 CL system: (a) H_2O_2 + luminol + cationic Au NCs; (b) H_2O_2 + luminol + Au NCs; (c) H_2O_2 + luminol + cationic BSA; (d) H_2O_2 + luminol + BSA; (e) H_2O_2 + luminol. (c) CL mechanisms of the luminol–H_2O_2 CL system catalyzed by cationic Au NCs. (Reprinted with permission from Han et al. (2018). Copyright 2018 John Wiley & Sons)

NCs surface provided higher affinity to the negatively charged luminol (Figure 3c). Inspired by this work, we expect that cationization of protein-protected MNCs or other nanozymes may become an effective way to enhance the enzymatic activity of nanozymes with negative charge.

In most cases, improvement of enzymatic activity is critical to the increase in sensitivity of enzyme-based biosensors. However, the inhibition of catalytic activity is also useful in enzyme-based biosensors (Tseng, Chang, Chang, & Huang, 2012). Zheng et al. discovered that the intrinsic peroxidase enzymatic activity of BSA-Au NCs can be inhibited by Hg^{2+} (Zhu et al., 2013). Hg^{2+} inhibits the enzymatic activity by specific interaction between Au^{+} and Hg^{2+} on the surface of BSA-Au NCs, changing the binding energy of Au^{+} that act as peroxidase activity sites. On the basis of the inhibiting function of Hg^{2+} on the peroxidase mimetic property of BSA-Au NCs, a new sensor for Hg^{2+} detection was proposed with high selectivity and a LOD of 3 nM (Figure 4a).

Ag^{+} was also found to inhibit the intrinsic peroxidase enzymatic property of BSA-Au NCs (Chang et al., 2016). After the addition of Ag^{+}, Ag^{+} selectively reacted with the Au core, causing its change from Ag^{+} to Ag^{0} and the generation of hybrid Au @ Ag NCs. The generated Au @ Ag NCs exhibited a weaker affinity to both H_2O_2 and TMB and lower enzymatic activity. Ground on this effect, a simple and feasible colorimetric sensor for Ag^{+} detection was developed.

For the first time, Song and coworkers observed inhibition and recovery of the peroxidase enzymatic activity of BSA-Au NCs by introduction of cysteine (Cys) and Hg^{2+} (Y.-W. Wang et al., 2016). They discovered that Cys can inhibit the enzymatic property of BSA-Au NCs by Au—SH interaction, because their thiol groups blocked the catalytic site of Au core, and the small amount of Au^{+} on the surface of the Au core, which contributed to stabilize the NCs was reduced. Nevertheless, the stronger interaction between Cys and $Hg^{2+}$was able to purge Cys from Au NCs surfaces in the presence of Hg^{2+} and subsequently restoring the catalytic activity of BSA-Au NCs. Based on this phenomenon, a simple and low-cost colorimetric method was developed for analysis of Cys and Hg^{2+} (Figure 4b). The assay results of water samples were basically consistent with inductively coupled plasma-mass spectrometry results, which proved the accuracy of this method.

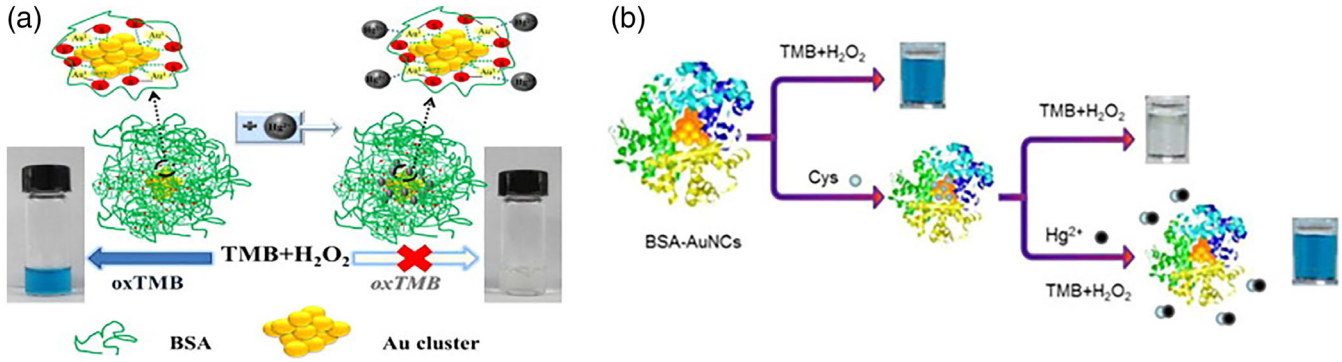

FIGURE 4 Detection methods based on the effect of substance on the peroxidase mimetic property of BSA-Au NCs. (a) Schematic diagram of Hg^{2+} detection. (Reprinted with permission from Zhu et al. (2013). Copyright 2013 Elsevier B.V.) (b) Schematic diagram of the colorimetric detection of Cys and Hg^{2+} by BSA-Au NCs. (Reprinted with permission from Y.-W. Wang et al. (2016). Copyright 2016 Elsevier B.V.)

In the work discussed above, proteins (e.g., BSA, lysozyme) act as the reductant and stabilizer for MNCs because of its biocompatibility and multiple binding sites for transition metal ions. Proteins can also provide a myriad of other functions according to its features. Wang and coworkers used apoferritin as a size-constrained reaction vessel for NC synthesis (Jiang et al., 2015). It has been reported that Au NCs can bind strongly with the histidine residues at the ferroxidase center of the H-submit of ferritin (Ueno et al., 2009). Therefore, apoferritin—which contains two H submits—enabled controllable catalysis of paired gold clusters (i.e., one cluster per H-submit) within the apoferritin nanocage (Figure 5a). The apoferritin-paired gold clusters (Au-Ft) possesses peroxidase mimetic property maintained at broad pH (0–12) and temperatures (4–70°C) (Figure 5b), which is associated with the high robustness of ferritin in comparison to BSA (K. L. Fan et al., 2012). Importantly, Au-Ft showed markedly higher catalytic activity toward TMB than 6 or 20 nm Au NPs (Table 2). This is contributed to the fact that ultra-small protein-protected MNCs have a higher surface-to-volume ratio to provide catalytic sites than large size NPs. Ueno et al. elucidated the detailed mechanism of formation of Au NCs within an apoferritin mutant: as Au ions gradually move toward the threefold channels center of apoferritin cage and form a sub-nanocluster, the conformation of the amino acid residues which bind to Au ions changes (Figure 5c). This results may help to understand the interactions between protein and metal ions and provide important insight for designing protein-protected MNCs (B. Maity et al., 2017).

Protamine (PRT) is natural protein in animal sperms which have high arginine content (Sivamani, DeLong, & Qu, 2009). Wang and coworkers employed PRT as both a stabilizer and a reducer to synthesize Au NCs (PRT-Au NCs) which can ensure controllable synthesis and biocompatibility (Y. Q. Huang et al., 2018). Interestingly, they found that not only did Hg^{2+} ions cause no inhibition on the enzymatic activity of PRT-Au NCs, the addition of Hg^{2+} can selectively enhance the peroxidase enzymatic activity of PRT-Au NCs (Figure 5d). They deduced that the enhancement process might contain two steps. First, Au^0/Au^+ on the PRT-Au NCs bind to the N atoms of arginine residues in protamine to form Au—N bond rather than Au—S bond in BSA-Au NCs. Second, Au—N bond facilitates the oxidation of Au^0/Au^+ to form the cationic Au species and the partly oxidized ionic Au species ($Au^{\delta+}$) in the presence of Hg^{2+}. Such cationic Au species and $Au^{\delta+}$ as peroxidase enzymatic active sites improve the surface properties of the PRT-Au NCs and enhance their enzymatical activity. On the basis of this finding, Wang and coworkers proposed a strategy for quantitative detection of Hg^{2+} via visual observation and UV-vis absorption. Owing to the fact that a small change in enzymatic activity could cause a dramatic effect on the chromogenic reaction, the proposed sensor is highly sensitive with a wide linear range and a LOD of 1.16 nM.

It is important to detect the concentration of free bilirubin in blood serum for assessing the risk caused by hyperbilirubemia in the event of neonatal jaundice (Wennberg, Ahlfors, Bhutani, Johnson, & Shapiro, 2006). Notably, bilirubin naturally evolves strong binding affinity to human serum albumin (HSA), with the binding constant at 2–13 times higher than that of BSA (Faerch & Jacobsen, 1975). In this regard, Goswami et al. proposed a sensitive and selective detection method for free bilirubin utilizing HSA protected Au NCs (HSA-Au NCs) as a fluorometric and colorimetric probe (Figure 5e; Santhosh et al., 2014). Due to the interaction between substrate bilirubin and HSA-Au NCs and the formation of non-fluorescent bilirubin-HSA-Au NCs complex, fluorescence quenching of the HSA-Au NCs in a concentration dependent manner was observed. In addition, as a peroxidase mimic, HSA-Au NCs can oxidize unbound bilirubin (with maximum absorbance at 440 nm) to almost colorless compounds by H_2O_2; while HSA bound bilirubin was protected from oxidation. Therefore, this probe can also determine the free bilirubin concentration by measuring the decrease in A_{440} in the presence of HSA-Au NCs and H_2O_2.

HAS-Au NCs as a dual fluorometric and colorimetric probe reflect the multifunctionality of nanozymes, which have not only enzymatic activity but also specific nanoscale properties such as fluorescence, magnetism, and photothermal effect.

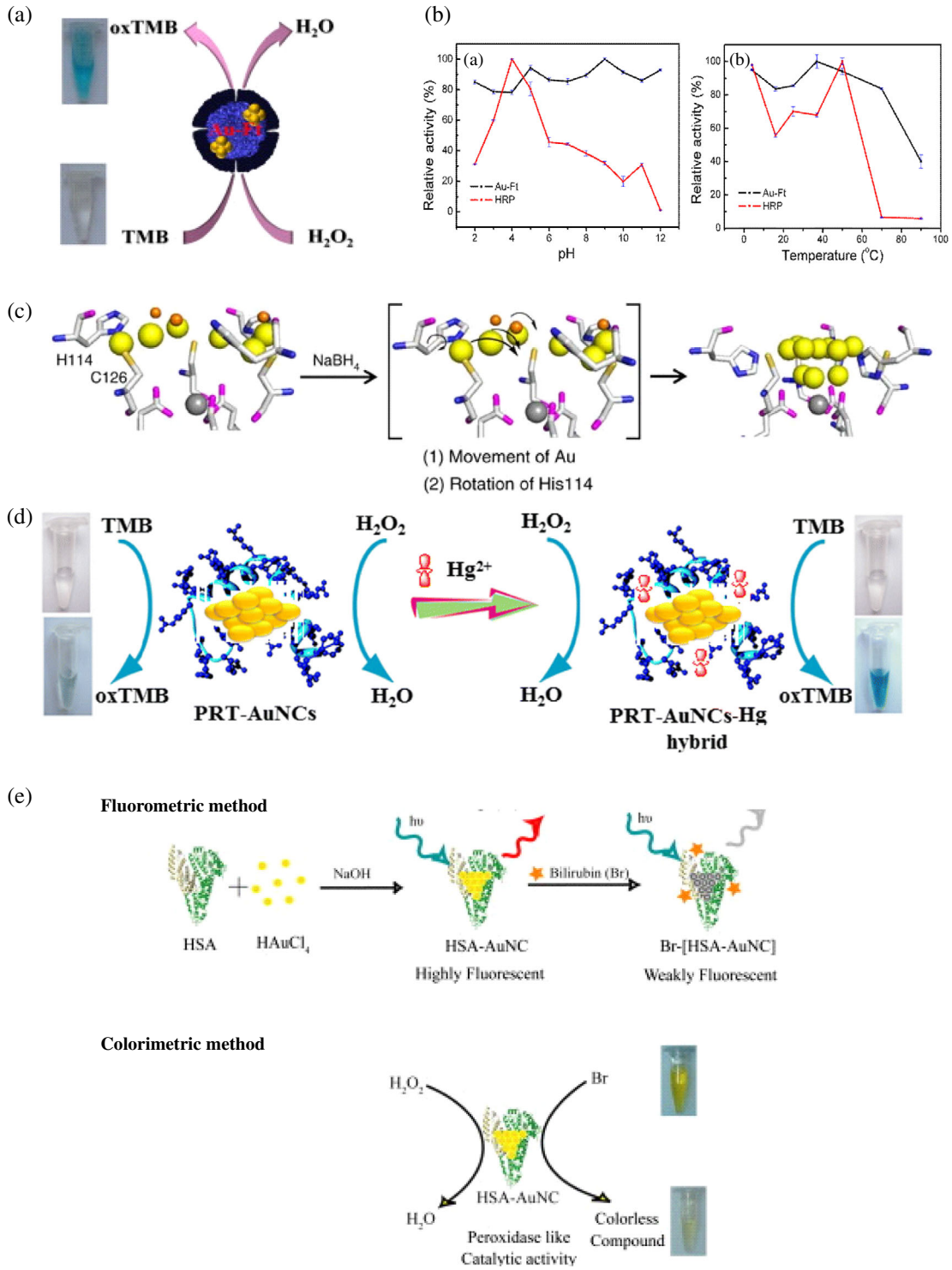

FIGURE 5 Protective proteins provide different functions in protein-protected MNCs nanozymes. (a) Prepared apoferritin-paired gold clusters. (b) Stability of Au-Ft and HRP. (Reprinted with permission from Jiang et al. (2015). Copyright 2015 Elsevier B.V.) (c) Formation of Au NCs at the threefold channel of apoferritin mutant. (Reprinted with permission from B. Maity, Abe, and Ueno (2017). Copyright 2017 Nature Publishing Group) (d) The colorimetric detection of Hg^{2+} using PRT-Au NCs as a nanozyme. (Reprinted with permission from Y. Q. Huang et al. (2018). Copyright 2018 Springer-Verlag GmbH Germany, part of Springer Nature) (e) Detection of free bilirubin by utilizing HSA-Au NCs as a fluorometric and colorimetric probe. (Reprinted with permission from Santhosh et al. (2014). Copyright 2014 Elsevier B.V.)

TABLE 2 Comparison of the catalytic activity of ultra-small Au-Ft and two large size Au NPs

Nanozymes	Size (nm)	Catalytic activity[a] (M/min)
Au-Ft	<2	4.37 ± 0.07
Au NPs	6	1.63 ± 0.13
Au NPs	20	0.989 ± 0.023

[a]Reaction condition: [TMB] = 300 mM, [H_2O_2] = 300 mM, [Nanozymes] = 0.58 μg/ml, in 0.2 M HOAc–NaOAc buffer at pH 4.0, at 45°C.

Synergistically combining the enzymatic activity with nanoscale properties can widen the application of protein-protected MNCs as well as nanozymes (Tao, Lin, Huang, et al., 2013). For example, taking advantages of high fluorescence and enzyme activity of BSA-Au NCs, Cai and coworkers constructed a fluorescence nanozyme probe on the basis of folate receptor-targeting Au NCs for tumor molecular colocalization diagnosis (D. Hu et al., 2014). Therefore, for the same tumor tissue, both fluorescent staining and peroxidase staining of the nanoprobes were obtained and the results were complementary to each other. This method efficiently avoids false-negative and false-positive results and further improves the specificity and accuracy of cancer diagnoses.

Owning to the high catalytic activity of Au NCs and functionalization of protective proteins, protein-protected Au NCs as peroxidase nanozymes have been widely used for in vitro molecular detection and disease diagnosis as mentioned above. In fact, they are also suitable for in vivo applications because of their ultra-small size and good biocompatibility. In this regard, Stevens and coworkers designed a protease-responsive sensor for in vivo disease monitoring by utilizing the peroxidase activity of peptide-protected Au NCs and their ultra-small size dependent tumor accumulation and renal clearance properties (Loynachan et al., 2019). The sensor was developed using biotinylated peptides which are the substrates of disease related proteases as protective ligands to synthesis the Au NCs nanozymes, which were then conjugated to neutravidin carrier. After reaching the site of disease, the sensor was disassembled in response to the dysregulated protease and the liberated Au NCs were filtered through the kidneys and into urine to produce a rapid and sensitive colorimetric readout of diseases state. By employing different enzymatic substrate as protective ligands for Au NCs, this modular approach will enable the rapid detection of a diverse range of diseases with dysregulated protease activities such as cancer, inflammation and thrombosis. This work would inspire researchers to pay more attention to the in vivo applications of protein-protected MNCs by utilizing their catalytic activities, fluorescence, renal clearance property and good biocompatibility.

2.2 | Peroxidase nanozymes based on protein-protected Pt NCs

Large size platinum (Pt) nanomaterials have been reported to exhibit four kinds of enzymatic activities including peroxidase, oxidase, catalase, and superoxide dismutase (Ma, Zhang, & Gu, 2011; Moglianetti et al., 2016). Therefore, great effort has been devoted to investigate how to control particle size and how it affects the enzymatic activities of Pt nanomaterials (Borodko et al., 2011).

Fu and coworkers chose BSA as the nucleation template to control the size of Pt-NCs. The prepared Pt-NCs showed the average diameter of 2 nm along with peroxidase-like activity (W. Li et al., 2015). Moreover, these ultra-small Pt-NCs showed higher initial velocities (v) in the oxidation of TMB in the presence of H_2O_2 than that of large size Pt NPs (Table 3). Therefore, ultra-small Pt-NCs possess higher peroxidase mimicking activity. The higher enzyme activity of the small size MNCs gives it an advantage over the large size ones.

Inspired by the work that metallophilic Hg^{2+}—Au^{+} interactions can efficiently inhibit the peroxidase enzymatic activity of BSA-Au NCs (Zhu et al., 2013), they investigated the interactions between Hg^{2+} and BSA-Pt NCs and the effect on enzymatic property. The results demonstrated that the addition of Hg^{2+} decreased the fraction of Pt^0 and in turn decreasing the enzymatic

TABLE 3 Comparison of the v in the oxidation of TMB in the presence of H_2O_2 catalyzed by ultra-small Pt NCs and large size Pt NPs

Nanozymes	Size (nm)	v^a (μM/s)
BSA-Pt NCs	2.00	0.11
BSA-Pt NPs	2.36	0.095
BSA-Pt NPs	2.43	0.08
BSA-Pt NPs	4.19	0.036

[a]Reaction condition: [TMB] = 125 μM, [H_2O_2] = 125 mM, [Pt] = 900 nM, in PBS buffer at pH 4.0, at 25°C.

activity of BSA-Pt NCs. Previous reports have shown that metallic Pt^0 of BSA-Pt takes part in the activation of substrate H_2O_2 to release •OH (Fu, Zhao, Zhang, & Li, 2014). Therefore, Fu and coworkers proposed that Hg^{2+} ions downregulated the peroxidase-like activity of BSA-Pt mainly through the interactions between Pt^0 and Hg^{2+}. On the basis of this phenomenon, they proposed a colorimetric Hg^{2+} sensing system, which was confirmed without significant interference from other metal ions. This is the first report to utilize Pt NCs for the detection of toxic metal ions.

2.3 | Peroxidase nanozymes based on protein-protected Cu NCs

Compared with the noble metals Au and Pt, Cu is relatively abundant, inexpensive, and readily available from commercial sources. In 2013, Xu et al. synthesized water-soluble Cu NCs by utilizing BSA as both a stabilizer and a reductant according to previous reports (Goswami et al., 2011). The BSA-Cu NCs were discovered to exhibit peroxidase enzymatic property for the first time and were applied for H_2O_2 and glucose assay (L. Hu et al., 2013).

However, literature also suggests that Cu NCs are difficult to maintain stable in aqueous solution because their surface are easy to be oxidized by air (R. Y. Li et al., 2016). To find a solution, Liao's group developed a simple one-pot method by utilizing BSA and dithiothreitol as stabilizer and reducer, respectively (Figure 6a). The Cu NCs showed water solubility and high stability in liquid solution. Furthermore, the Cu NCs showed excellent peroxidase enzymatic activity with a higher affinity to TMB than that of HRP. Combining this enzyme activity with the oxidation of xanthine by xanthine oxidase, a colorimetric sensor for xanthine detection was proposed by Liao's group (Yan et al., 2017).

Additionally, Xu et al. have discovered that BSA-Cu NCs could serve as a peroxidase nanozyme which greatly enhances the CL of the luminol–H_2O_2 (Xu et al., 2014). Then, they established a selective and sensitive CL sensor for the detection of cholesterol (Figure 6b). This sensor has been successfully applied to the determination of cholesterol in milk and human serum

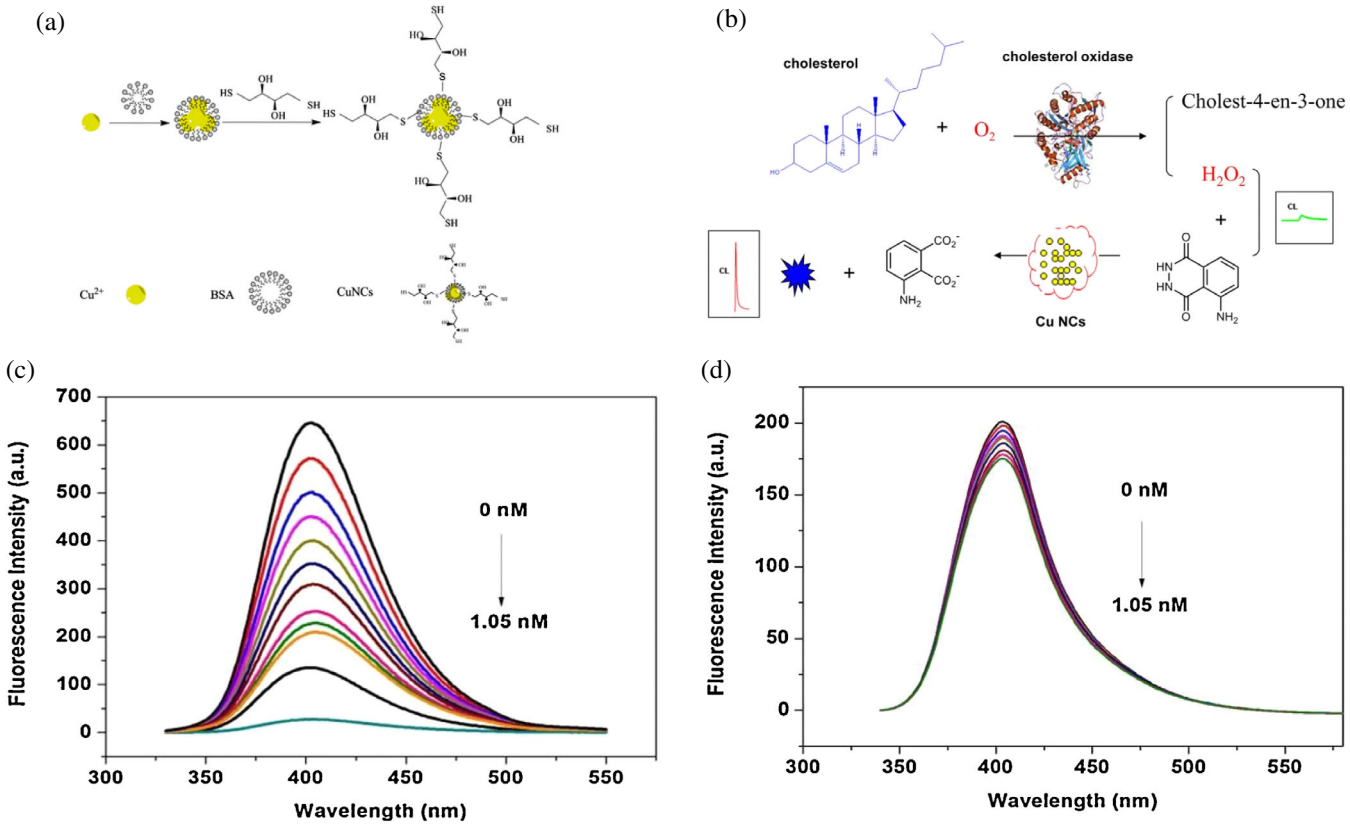

FIGURE 6 The preparation of protein-protected Cu NCs as peroxidase nanozymes and their application. (a) The scheme of stable BSA-Cu NCs preparation. (Reprinted with permission from Yan et al. (2017). Copyright 2017 Springer Science Business Media) (b) Principle of the BSA-Cu NCs-based chemiluminescence sensor for cholesterol. (Reprinted with permission from Xu et al. (2016). Copyright 2016 Nature Publishing Group) (c, d) The fluorescence response of BSA-Cu NC1 and BSA-Cu NC2 toward different concentrations of dopamine. (Reprinted with permission from Aparna et al. (2019). Copyright 2019 Elsevier B.V.)

with satisfactory precision and accuracy (Xu et al., 2016). This detection method widens the applications of protein-protected MNCs in the field of CL-based sensors.

Given that protein-protected MNCs have both enzyme activities and fluorescence properties, it is interesting to investigate whether these two properties affect each other and what effect might have on the application of protein-protected MNCs. George's group synthesized two kinds of blue emitting BSA-Cu NCs in presence (BSA-Cu NCs 1) and absence (BSA CuNCs 2) of H_2O_2 used for the detection of dopamine. They found that BSA-Cu NCs 1 showed rapid and high fluorescence quenching after addition of dopamine, while BSA-Cu NCs 2 showed slow and low response (Figure 6c,d). The fast response of BSA-Cu NCs 1 toward dopamine can be ascribed to the peroxidase activity of BSA-Cu NCs in the presence of H_2O_2, which results in the oxidation of dopamine to fluorescence quencher dopaquinone (Manini, Panzella, Napolitano, & d'Ischia, 2003). Therefore, a rapid and sensitive detection method for dopamine using BSA-Cu NCs 1 was established with a LOD of 0.1637 pM, while the method based on BSA-Cu NCs 2 was slower with a higher LOD of 0.024 nM (Aparna et al., 2019). These results proved that the enzymatic activity of protein-protected MNCs can affect the rapidity and sensitivity of fluorescence-based detection method.

3 | OXIDASE NANOZYMES BASED ON PROTEIN-PROTECTED MNCS

Oxidases are enzymes that catalyze the oxidation of substrate to an oxidized product by molecular oxygen (O_2), which acts as an electron acceptor and is reduced to H_2O or H_2O_2 (He, Wamer, Xia, Yin, & Fu, 2014). Oxidases can not only oxidize certain substrates with the result of a color change, but also degrade some pollutants by oxidation, which make them ideal agents for chemical sensors and environmental treatment. Recent studies have found that some protein-protected MNCs exhibit intrinsic oxidase enzymatic activity and as promising oxidase candidates for applications.

3.1 | Oxidase nanozymes based on protein-protected Au NCs

Wang et al. reported a novel oxidase mimetic based on the photochemical property of BSA-Au NCs. They found that BSA-Au NCs possessed oxidase enzymatic activity under visible light irradiation ($\lambda \geq 400$ nm), but showed almost no enzymatic property without light (G. L. Wang, Jin, Dong, Wu, & Li, 2015). Under the stimulation of visible light, BSA-Au NCs catalyzed the oxidation of TMB to the colored product without using H_2O_2 as an oxidant. In order to elucidate the enzymatic mechanism of BSA-Au NCs under visible light stimulation, a series of quenchers were used to remove the related active substances in the catalytic system, including superoxide anion ($O_2^{\bullet -}$), photo-generated holes (h^+), and hydroxyl radicals (•OH). According to the results, they concluded that the BSA-Au NCs can absorb visible light and produce electron (e^-)–hole (h^+) pairs that reacted with water or oxygen molecules to form active substances such as $O_2^{\bullet -}$and •OH. The generated •OH and $O_2^{\bullet -}$ then oxidizes the TMB (Figure 7a).

Based on the oxidase activity of BSA-Au NCs, Wang et al. developed a novel colorimetric sensor for the detection of trypsin (Figure 7b). In the presence of trypsin, the protein template of BSA-Au NCs was degraded and their catalytic activity was inhibited because the surface state of Au NCs changed and aggregated after BSA degradation. Using this system, as low as 0.6 μg/ml trypsin can be detected. This study provides a novel oxidase mimic based on the photochemical property of BSA-Au NCs, which encourages more experimental and theoretical studies on the relationship between enzymatic and photochemical properties.

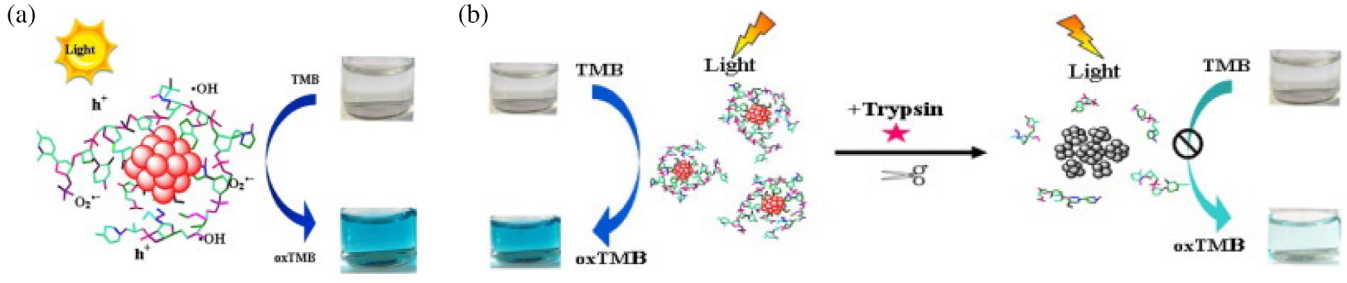

FIGURE 7 Oxidase nanozymes based on BSA-Au NCs and its intriguing application. (a) The catalytic reaction mechanism of the photoactivated oxidase enzymatic activity of BSA-Au NCs. (b) The colorimetric trypsin detection method based on the oxidase property of BSA-Au NCs. (Reprinted with permission from G. L. Wang et al. (2015). Copyright 2015 Elsevier B.V.)

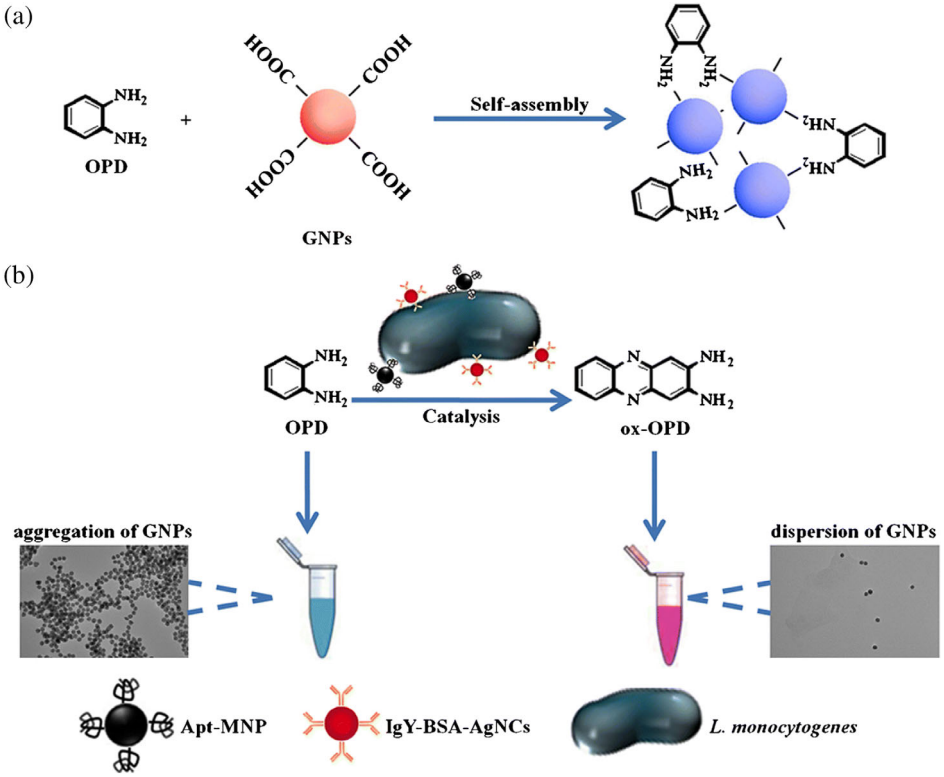

FIGURE 8 Schematic diagram of the colorimetric detection of *L. monocytogenes* based on the oxidase activity of BSA-Ag NCs. (a) GNPs aggregate in the presence of OPD. (b) The Ig Y-BSA-Ag NCs attached onto the sandwich-type complex can catalyze the oxidization of OPD to ox-OPD, which results in the disaggregation of GNPs. (Reprinted with permission from Liu et al. (2018). Copyright 2018 Springer-Verlag GmbH Austria, part of Springer Nature)

3.2 | Oxidase nanozymes based on protein-protected Ag NCs

Listeria monocytogenes which have low infectious dose (1,000 colony forming units, cfu) and can survive at refrigeration temperature, is considered as one of the most dangerous foodborne pathogens (Cole, Jones, & Holyoak, 1990). As a result, it is important to develop simple methods for detecting *L. monocytogenes* in food samples (Silk, McCoy, Iwamoto, & Griffin, 2014).

Based on the study that Ag^+ and Ag^0 can both trigger and accelerate the oxidation of *o*-phenylenediamine (OPD) (X. Yang & Wang, 2011), Vosch and Yang synthesized BSA-Ag NCs containing Ag^+ and Ag^0 as oxidase nanozymes. By using core gold nanoparticles (GNPs), BSA-Ag NCs as oxidase mimics, they proposed a rapid detection method for *L. monocytogenes* on the basis of OPD-mediated disaggregation of GNPs (Liu et al., 2018). As shown in Figure 8a, GNPs aggregate in the presence of OPD with accompanying a color change from red to blue, with peaks of 525 and 730 nm, respectively. This OPD-mediated aggregation of GNPs was used as the reporting system. Sandwich complexes "magnetic beads modified with aptamer, *L. monocytogenes*, immunoglobulin Y (IgY) antibody-coated BSA-Ag NCs" was formed. After a simple magnetic separation, the BSA-Ag NCs attached onto the sandwich-type immunocomplex can oxidize OPD and cause the disaggregation of GNPs, and the change in color from blue to red were directly proportional to the bacteria concentration (Figure 8b). Taking advantages of the superior catalytic activity of BSA-Ag NCs, as *L. monocytogenes* of a wide range from 10 to 10^6 cfu/ml and a LOD of 10 cfu/ml can be detected with. This work expands the application of oxidase nanozymes based on protein-protected MNCs in analytical chemistry.

3.3 | Oxidase nanozymes based on protein-protected Pt NCs

Tseng and coworkers presented a simple, one-pot route for the synthesis of Pt NCs utilizing lysozyme (Lys) as a protective ligand (C. J. Yu et al., 2014). They found that the Lys-Pt NCs exhibited oxidase enzymatic activity because Pt NCs can catalyze the oxidation of organic substrates such as TMB, ABTS and dopamine by O_2 (Figure 9a). In addition, they examined the oxidation of ABTS by some larger size NPs (Figure 9b). The results showed the catalytic activities follow the trend Lys-Pt NCs > Pt NPs (5 nm) > Pt NPs (30 nm) > Lys > Au NPs (13 nm) > HRP > Fe_3O_4 NPs (13 nm), suggesting the high catalytic activity of ultra-small Lys-Pt NCs. They proposed that the mechanism of Lys-Pt NCs-catalyzed oxidation of organic substrates is a four-electron reduction process [$O_2(g) + 4H^+(aq) + 4e^- \rightarrow 2H_2O(l)$], in which dissolved organic substrates and O_2 act as electron donors and electron acceptors, respectively. The oxidase enzymatic property of Lys-Pt NCs motivated Tseng

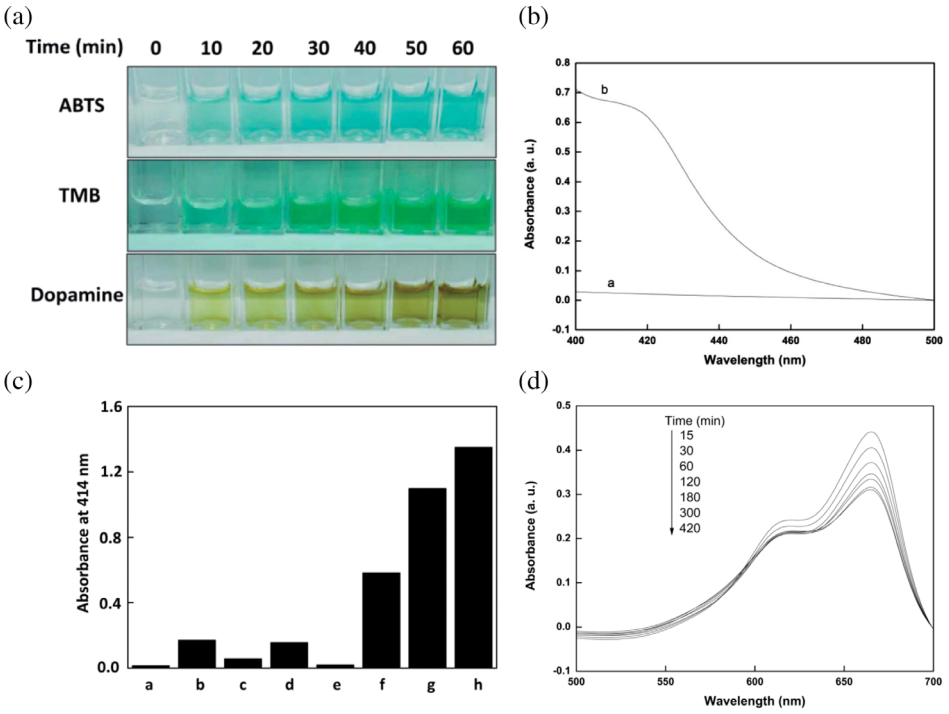

FIGURE 9 Lys-Pt NCs as an oxidase nanozyme and its application for degrading environmental pollutants. (a) Lys-Pt NCs catalyze the oxidation of organic substrates such as TMB, ABTS and dopamine by O_2. (b) Absorption spectra of oxidized ABTS catalyzed by Pt NCs under (a) N_2 saturated and (b) aerobic conditions. (c) Absorption spectra of oxidized ABTS obtained in the absence (a) and presence of (b) Lys, (c) HRP, (d) 13 nm Au NPs, (e) 13 nm Fe_3O_4 NPs, (f) 30 nm Pt NPs, (g) 5 nm Pt NPs, and (h) Lys-Pt NCs. (d) After the addition of Lys-Pt NCs, the 665 nm maximal absorbance of methylene blue in lake water samples gradually decreases. (Reprinted with permission from C. J. Yu et al. (2014). Copyright 2014 Royal Society of Chemistry)

and coworkers to utilize the Pt NCs to the oxidative degradation of pollutants in environmental water. After the addition of Pt NCs, the 665 nm maximal absorbance of methylene blue in lake water samples gradually decreased (Figure 9b). Compared to peroxidase-like nanozymes in degrading environmental pollutants, this system is friendly because it avoids the high concentration of toxic H_2O_2.

4 | CATALASE NANOZYMES BASED ON PROTEIN-PROTECTED MNCS

Catalase is enzyme that catalyze the decomposition of hydrogen peroxide into molecular oxygen and water. In biological systems, hydrogen peroxide serves as a signaling molecule or a nonradical reactive oxygen species (Karakoti et al., 2010). Catalase is employed as the most efficient enzyme for the conversion of hydrogen peroxide to less active oxygen. Inspired by its remarkably catalytic efficiency, researchers have long sought to develop alternative materials such as protein-protected MNCs that would mimic the catalytic activity of catalase.

Using apoferritin (apoFt) as a protective ligand, Nie and Zhao achieved successful synthesis of 1–2 nm Pt NCs, which were highly stable (Figure 10a; J. Fan et al., 2011). The result Pt-Ft showed the ability to reduce the DEPMPO/$OH^{\cdot}$ adduct signal intensity in H_2O_2/UV DEPMPO spin trap system similar to catalase (Figure 10b), which means that Pt-Ft can decrease the concentration of H_2O_2. Moreover, gas bubbles were also observed in the capillary tubes which contain Pt-Ft or catalase (Figure 10c). Both phenomena indicated that Pt-Ft has catalase enzymatic activity (J. Fan et al., 2011). Then, they found that for the catalase activity of Pt-Ft, the optimal pH is 12 and the optimal temperature is 85°C. The catalytic activity of Pt-Ft is much more stable than natural catalase, supported by the result that Pt-Ft retained its activity at all temperatures (4–85°C), while catalase almost had no activity above 60°C.

In the synthesis process, apoferritin act as a nanoreactor to control the size of Pt NCs. It has been reported that histidine residues can bind Pt ion with high affinity (Dickerson et al., 2008), so the limited potential binding sites in ferritin (six histidine residues in each Ft light chain) become one of the factors limiting the core size of Pt-Ft. This explained the phenomenon that increasing the Pt-to-apoferritin ratio to 30 (atoms per molecule) in the synthesis process caused the generation of large Pt NPs outside the apoferritin.

Taken together, this study showed the feasibility of utilizing apoferritin as a protective protein to control the synthesis of Pt NCs, and the as-prepared Pt-Ft showed catalase-like activity. This catalase mimic may be employed as a substitute of catalase in various human diseases which involve oxidative stress damage.

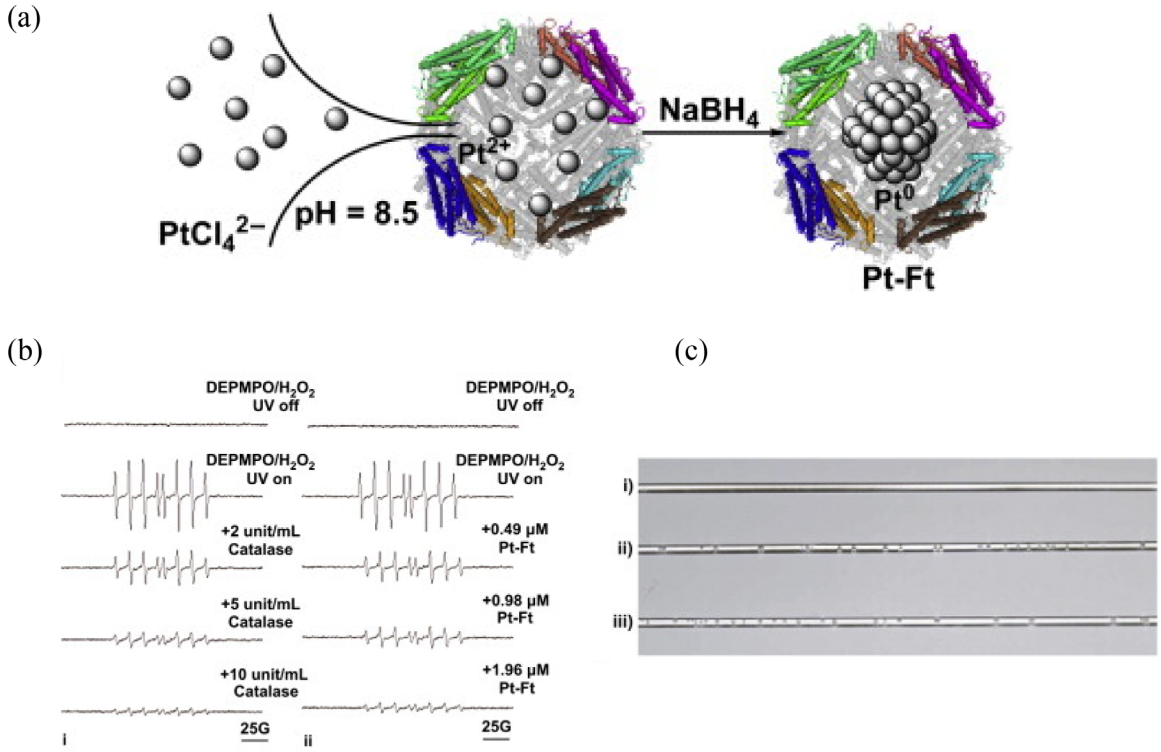

FIGURE 10 Catalase enzymatic activity of ferritin-Ft NCs. (a) Schematic diagram of the synthesis method of Pt-Ft. (b) The effects of catalase (i) and Pt-Ft (ii) on H_2O_2/UV system. (c) Gas bubbles were observed in the quartz capillary tubes after the UV/H_2O_2 with catalase/Pt-Ft experiment. (Reprinted with permission from J. Fan et al. (2011). Copyright 2011 Elsevier)

5 | CONCLUSION

From our review, we can see that the enzyme catalytic activity of protein-protected MNCs has been previously overlooked but is now getting more and more attention. Many protein-protected MNCs have demonstrated intrinsic peroxidase, oxidase and catalase activities and have thus been used for biological analysis and environmental treatment. These findings have extended the horizon of protein-protected MNCs' properties as well as their application in various fields. Furthermore, in the field of nanozymes, protein-protected MNCs have emerged as an outstanding new addition—ultra-small (<2 nm) nanozymes.

Compared to large size (>2 nm) nanozymes, ultra-small protein-protected MNCs nanozymes are more competent for biomedical applications due to the following advantages: (a) they usually have higher catalytic activity than larger NPs because of their greater surface-to-volume ratio to interact with substrates (W. Li et al., 2015); (b) the ultra-small sizes which are smaller than the renal threshold (<5.5 nm) (Derfus, Chan, & Bhatia, 2004) make them easier to expel from the body and increase the potential of in vivo application; (c) protein-protected MNCs give us the best of two worlds, where we are able to exploit the nanoscale behavior of the MNCs as well as the biocompatibility and bioactivity of the protein to develop methods in diagnostic and therapeutic applications; (d) protein-protected MNCs have not only enzymatic activity but also strong photoluminescence, synergistically combining these two properties will widen the application of ultra-small protein-protected MNCs nanozymes.

Despite the above advantages and advanced progress in the development of protein-protected MNCs as ultra-small nanozymes, there are still following challenges that need to be addressed in future work:

1. Although recent advances have enabled facile synthesis of water-soluble, protein-protected MNCs, most researchers still only rely on BSA as both the reducing agent and stabilizer that could ensure biocompatibility and protection from aggregation. As we know, protein-protected MNCs may retain the bioactivity of the protein ligand, which may offer its own features to the result MNCs (W. Y. Chen et al., 2010). Therefore, it is necessary to explore methods for synthesizing other new protein-protected MNCs. The new protein-protected MNCs may exhibit unique and excellent properties, which will widen the diagnostic and therapeutic applications of protein-protected MNCs nanozymes.

2. In nature, there are six types of catalytic reactions: oxidoreductases, transferases, hydrolases, isomerases, ligases, and lyases. Thus far, although many protein-protected MNCs have demonstrated enzyme activities, they all are oxidoreductase-like activities such as peroxidase, oxidase, and catalase. Therefore, there is a vast room for developing other types of nanozymes based on protein-protected MNCs. In this regard, more understanding of the structures and catalytic mechanisms of protein-protected MNCs is required in addition to the deeper understanding on natural enzymes themselves.
3. As known to all, nanozymes based on protein-protected MNCs have advantages compared to natural enzymes in regards to their high stability and low cost. However, their catalytic activity and affinity toward substrate such as H_2O_2 still cannot compete with natural enzymes. The solution may be to learn from the catalytic mechanism of natural enzymes to find a feasible strategy of modification for nanozymes including protein-protected MNCs. For example, modification with a single amino acid mimicking the enzymatic microenvironment of natural peroxidase could improve by more than 10-fold the apparent affinity of the Fe_3O_4 nanozyme toward H_2O_2 and enhance its enzymatic activity up to 20-fold (K. L. Fan et al., 2017). This new rationale for improving the activity of nanozyme is also available for nanozymes based on protein-protected MNCs.
4. Up to now, a considerable number of reports have suggested that ultra-small nanozymes based on protein-protected MNCs are promising tools for biological analysis. However, little is known about the therapeutic function of these ultra-small clusters in vivo despite their advantages of suitable size and good biocompatibility for in vivo applications. It is well known that peroxidase, oxidase and catalase are main enzymes in biological systems involved in the maintenance of redox homeostasis. Thus, more attention should be paid to the usage of these ultra-small nanozymes based on protein-protected MNCs as bio-catalysts in various human diseases involved in redox dysregulation such as cancer, inflammation, cardiovascular diseases. It is also possible to employ the products of redox nanozymes to treat other diseases, for example, use the toxic hydroxyl radicals produced by peroxidase nanozymes to treat bacterial infection.

Overall, there is still much room for future research and application of ultra-small nanozymes based on protein-protected MNCs. We expect that the enzyme-like activity of protein-protected MNCs will certainly attract broader interests across various disciplines and stimulate research in the fields of nanotechnology and biology, making these emerging ultra-small nanozymes become novel multifunctional nanomaterials for a number of biomedical applications.

ACKNOWLEDGMENTS

This work was financially supported by the National Natural Science Foundation of China (No. 31530026, 31900981, 31871005), Chinese Academy of Sciences under Grant No. YJKYYQ20180048, the Strategic Priority Research Program (XDPB29040101), the Key Research Program of Frontier Sciences, CAS (Grant No. QYZDY-SSW-SMC013), National Key Research and Development Program of China (No. 2017YFA0205501) and Youth Innovation Promotion Association CAS (No. 2019093).

CONFLICT OF INTEREST

The authors have declared no conflicts of interest for this article.

AUTHOR CONTRIBUTIONS

Xiangqin Meng: Conceptualization; data curation; formal analysis; funding acquisition; investigation; methodology; project administration; resources; software; supervision; validation; visualization; writing-original draft; writing-review and editing. **Iman Zare**: Conceptualization; data curation; formal analysis; funding acquisition; investigation; methodology; project administration; resources; software; supervision; validation; visualization; writing-original draft; writing-review and editing. **Xiyun Yan**: Conceptualization; data curation; formal analysis; funding acquisition; investigation; methodology; project administration; resources; software; supervision; validation; visualization; writing-original draft; writing-review and editing. **Kelong Fan**: Conceptualization; data curation; formal analysis; funding acquisition; investigation; methodology; project administration; resources; software; supervision; validation; visualization; writing-original draft; writing-review and editing.

ORCID

Kelong Fan https://orcid.org/0000-0001-6285-1933

RELATED WIRES ARTICLES

Ultrasmall metal nanoclusters for bio-related applications
Gold nanoclusters with enhanced tunable fluorescence as bioimaging probes

REFERENCES

Ahmed, S., Kishikawa, N., Ohyama, K., Maki, T., Kurosaki, H., Nakashima, K., & Kuroda, N. (2009). An ultrasensitive and highly selective determination method for quinones by high-performance liquid chromatography with photochemically initiated luminol chemiluminescence. *Journal of Chromatography A*, *1216*(18), 3977–3984.

Aparna, R. S., Devi, J. S. A., Nebu, J., Syamchand, S. S., & George, S. (2019). Rapid response of dopamine towards in situ synthesised copper nanocluster in presence of H_2O_2. *Journal of Photochemistry and Photobiology, A: Chemistry*, *379*, 63–71. https://doi.org/10.1016/j.jphotochem.2019.04.043

Borodko, Y., Thompson, C. M., Huang, W. Y., Yildiz, H. B., Frei, H., & Somorjai, G. A. (2011). Spectroscopic study of platinum and rhodium dendrimer (PAMAM G4OH) compounds: Structure and stability. *Journal of Physical Chemistry C*, *115*(11), 4757–4767.

Chang, Y., Zhang, Z., Hao, J., Yang, W., & Tang, J. (2016). BSA-stabilized Au clusters as peroxidase mimetic for colorimetric detection of Ag^+. *Sensors and Actuators B: Chemical*, *232*, 692–697. https://doi.org/10.1016/j.snb.2016.04.039

Chen, Q. Y., Li, D. H., Zhu, Q. Z., Yang, H. H., Zheng, H., & Xu, J. G. (2000). Investigation on the potential use of the mimetic peroxidase-catalyzed reaction of hydrogen peroxide and *o*-hydroxyphenylfluorone in fluorescence analysis. *Analytica Chimica Acta*, *406*(2), 209–215.

Chen, W. Y., Lin, J. Y., Chen, W. J., Luo, L. Y., Diau, E. W. G., & Chen, Y. C. (2010). Functional gold nanoclusters as antimicrobial agents, for antibiotic-resistant bacteria. *Nanomedicine*, *5*(5), 755–764.

Chevrier, D. M., Chatt, A., & Zhang, P. (2012). Properties and applications of protein-stabilized fluorescent gold nanoclusters: Short review. *Journal of Nanophotonics*, *6*(1), 064504. https://doi.org/10.1117/1.JNP.6

Cho, S., Shin, H. Y., & Kim, M. I. (2017). Nanohybrids consisting of magnetic nanoparticles and gold nanoclusters as effective peroxidase mimics and their application for colorimetric detection of glucose. *Biointerphases*, *12*(1), 01A401. https://doi.org/10.1116/1.4974198

Cole, M. B., Jones, M. V., & Holyoak, C. (1990). The effect of pH, salt concentration and temperature on the survival and growth of listeria-monocytogenes. *Journal of Applied Bacteriology*, *69*(1), 63–72.

Cui, M., Zhao, Y., & Song, Q. (2014). Synthesis, optical properties and applications of ultra-small luminescent gold nanoclusters. *TrAC Trends in Analytical Chemistry*, *57*, 73–82. https://doi.org/10.1016/j.trac.2014.02.005

Deng, M., Xu, S., & Chen, F. (2014). Enhanced chemiluminescence of the luminol-hydrogen peroxide system by BSA-stabilized Au nanoclusters as a peroxidase mimic and its application. *Analytical Methods*, *6*(9), 3117–3123. https://doi.org/10.1039/c3ay42135j

Derfus, A. M., Chan, W. C. W., & Bhatia, S. N. (2004). Probing the cytotoxicity of semiconductor quantum dots. *Nano Letters*, *4*(1), 11–18. https://doi.org/10.1021/nl0347334

Dickerson, M. B., Sandhage, K. H., & Naik, R. R. (2008). Protein- and peptide-directed syntheses of inorganic materials. *Chemical Reviews*, *108*(11), 4935–4978. https://doi.org/10.1021/cr8002328

Dong, Y. L., Zhang, H. G., Rahman, Z. U., Su, L., Chen, X. J., Hu, J., & Chen, X. G. (2012). Graphene oxide-Fe_3O_4 magnetic nanocomposites with peroxidase-like activity for colorimetric detection of glucose. *Nanoscale*, *4*(13), 3969–3976. https://doi.org/10.1039/c2nr12109c

Faerch, T., & Jacobsen, J. (1975). Determination of association and dissociation rate constants for bilirubin bovine serum-albumin. *Archives of Biochemistry and Biophysics*, *168*(2), 351–357.

Fan, J., Yin, J. J., Ning, B., Wu, X., Hu, Y., Ferrari, M., … Nie, G. (2011). Direct evidence for catalase and peroxidase activities of ferritin-platinum nanoparticles. *Biomaterials*, *32*(6), 1611–1618. https://doi.org/10.1016/j.biomaterials.2010.11.004

Fan, K. L., Cao, C. Q., Pan, Y. X., Lu, D., Yang, D. L., Feng, J., … Yan, X. Y. (2012). Magnetoferritin nanoparticles for targeting and visualizing tumour tissues. *Nature Nanotechnology*, *7*(7), 459–464.

Fan, K. L., Wang, H., Xi, J. Q., Liu, Q., Meng, X. Q., Duan, D. M., … Yan, X. Y. (2017). Optimization of Fe_3O_4 nanozyme activity via single amino acid modification mimicking an enzyme active site. *Chemical Communications*, *53*(2), 424–427.

Fu, Y., Zhao, X. Y., Zhang, J. L., & Li, W. (2014). DNA-based platinum nanozymes for peroxidase mimetics. *Journal of Physical Chemistry C*, *118*(31), 18116–18125.

Gao, L., & Yan, X. (2016). Nanozymes: An emerging field bridging nanotechnology and biology. *Science China. Life Sciences*, *59*(4), 400–402. https://doi.org/10.1007/s11427-016-5044-3

Gao, L.-Z., & Yan, X.-Y. (2013). Discovery and current application of nanozyme. *Acta Agronomica Sinica*, *40*(10), 892. https://doi.org/10.3724/sp.j.1206.2013.00409

Gao, L. Z., Zhuang, J., Nie, L., Zhang, J. B., Zhang, Y., Gu, N., … Yan, X. (2007). Intrinsic peroxidase-like activity of ferromagnetic nanoparticles. *Nature Nanotechnology*, *2*(9), 577–583.

Goswami, N., Giri, A., Bootharaju, M. S., Xavier, P. L., Pradeep, T., & Pal, S. K. (2011). Copper quantum clusters in protein matrix: Potential sensor of Pb^{2+} ion. *Analytical Chemistry*, *83*(24), 9676–9680.

Han, L., Li, Y., & Fan, A. (2018). Improvement of mimetic peroxidase activity of gold nanoclusters on the luminol chemiluminescence reaction by surface modification with ethanediamine. *Luminescence*, *33*(4), 751–758. https://doi.org/10.1002/bio.3472

He, W. W., Liu, Y., Yuan, J. S., Yin, J. J., Wu, X. C., Hu, X. N., … Guo, Y. T. (2011). Au@Pt nanostructures as oxidase and peroxidase mimetics for use in immunoassays. *Biomaterials*, *32*(4), 1139–1147. https://doi.org/10.1016/j.biomaterials.2010.09.040

He, W. W., Wamer, W., Xia, Q. S., Yin, J. J., & Fu, P. P. (2014). Enzyme-like activity of nanomaterials. *Journal of Environmental Science and Health Part C*, *32*(2), 186–211.

Hu, D., Sheng, Z., Fang, S., Wang, Y., Gao, D., Zhang, P., … Cai, L. (2014). Folate receptor-targeting gold nanoclusters as fluorescence enzyme mimetic nanoprobes for tumor molecular colocalization diagnosis. *Theranostics*, *4*(2), 142–153. https://doi.org/10.7150/thno.7266

Hu, L., Yuan, Y., Zhang, L., Zhao, J., Majeed, S., & Xu, G. (2013). Copper nanoclusters as peroxidase mimetics and their applications to H_2O_2 and glucose detection. *Analytica Chimica Acta*, *762*, 83–86. https://doi.org/10.1016/j.aca.2012.11.056

Huang, Y., Ren, J., & Qu, X. (2019). Nanozymes: Classification, catalytic mechanisms, activity regulation, and applications. *Chemical Reviews*, *119*(6), 4357–4412. https://doi.org/10.1021/acs.chemrev.8b00672

Huang, Y. Q., Fu, S., Wang, Y. S., Xue, J. H., Xiao, X. L., Chen, S. H., & Zhou, B. (2018). Protamine-gold nanoclusters as peroxidase mimics and the selective enhancement of their activity by mercury ions for highly sensitive colorimetric assay of Hg(II). *Analytical and Bioanalytical Chemistry*, *410*(28), 7385–7394. https://doi.org/10.1007/s00216-018-1344-8

Jiang, X., Sun, C., Guo, Y., Nie, G., & Xu, L. (2015). Peroxidase-like activity of apoferritin paired gold clusters for glucose detection. *Biosensors and Bioelectronics*, *64*, 165–170. https://doi.org/10.1016/j.bios.2014.08.078

Jin, R. C. (2010). Quantum sized, thiolate-protected gold nanoclusters. *Nanoscale*, *2*(3), 343–362. https://doi.org/10.1039/b9nr00160c

Karakoti, A., Singh, S., Dowding, J. M., Seal, S., & Self, W. T. (2010). Redox-active radical scavenging nanomaterials. *Chemical Society Reviews*, *39*(11), 4422–4432. https://doi.org/10.1039/b919677n

Kricka, L. J. (1995). Chemiluminescence and bioluminescence. *Analytical Chemistry*, *67*(12), R499–R502.

Li, C. G., Chen, H., Chen, B., & Zhao, G. H. (2018). Highly fluorescent gold nanoclusters stabilized by food proteins: From preparation to application in detection of food contaminants and bioactive nutrients. *Critical Reviews in Food Science and Nutrition*, *58*(5), 689–699. https://doi.org/10.1080/10408398.2016.1213698

Li, H., Zhu, W., Wan, A., & Liu, L. (2017). The mechanism and application of the protein-stabilized gold nanocluster sensing system. *Analyst*, *142*(4), 567–581. https://doi.org/10.1039/c6an02112c

Li, M. Q., Lao, Y. H., Mintz, R. L., Chen, Z. G., Shao, D., Hu, H. Z., … Leong, K. W. (2019). A multifunctional mesoporous silica-gold nanocluster hybrid platform for selective breast cancer cell detection using a catalytic amplification-based colorimetric assay. *Nanoscale*, *11*(6), 2631–2636. https://doi.org/10.1039/c8nr08337a

Li, R. Y., Wang, H. Y., Zhou, X. Y., Liao, X. Q., Sun, X. L., & Li, Z. J. (2016). D-Penicillamine and bovine serum albumin co-stabilized copper nanoclusters with remarkably enhanced fluorescence intensity and photostability for ultrasensitive detection of Ag^{+}. *New Journal of Chemistry*, *40*(1), 732–739.

Li, W., Chen, B., Zhang, H., Sun, Y., Wang, J., Zhang, J., & Fu, Y. (2015). BSA-stabilized Pt nanozyme for peroxidase mimetics and its application on colorimetric detection of mercury(II) ions. *Biosensors and Bioelectronics*, *66*, 251–258. https://doi.org/10.1016/j.bios.2014.11.032

Liu, Y., Wang, J., Song, X., Xu, K., Chen, H., Zhao, C., & Li, J. (2018). Colorimetric immunoassay for *Listeria monocytogenes* by using core gold nanoparticles, silver nanoclusters as oxidase mimetics, and aptamer-conjugated magnetic nanoparticles. *Mikrochimica Acta*, *185*(8), 360. https://doi.org/10.1007/s00604-018-2896-1

Loynachan, C. N., Soleimany, A. P., Dudani, J. S., Lin, Y., Najer, A., Bekdemir, A., … Stevens, M. M. (2019). Renal clearable catalytic gold nanoclusters for in vivo disease monitoring. *Nature Nanotechnology*, *14*(9), 883–890. https://doi.org/10.1038/s41565-019-0527-6

Lu, Y. Z., & Chen, W. (2012). Sub-nanometre sized metal clusters: From synthetic challenges to the unique property discoveries. *Chemical Society Reviews*, *41*(9), 3594–3623. https://doi.org/10.1039/c2cs15325d

Ma, M., Zhang, Y., & Gu, N. (2011). Peroxidase-like catalytic activity of cubic Pt nanocrystals. *Colloids and Surfaces. A, Physicochemical and Engineering Aspects*, *373*(1–3), 6–10.

Maity, B., Abe, S., & Ueno, T. (2017). Observation of gold sub-nanocluster nucleation within a crystalline protein cage. *Nature Communications*, *8*, 14820. https://doi.org/10.1038/ncomms14820

Maity, P., Xie, S. H., Yamauchi, M., & Tsukuda, T. (2012). Stabilized gold clusters: From isolation toward controlled synthesis. *Nanoscale*, *4*(14), 4027–4037. https://doi.org/10.1039/c2nr30900a

Manini, P., Panzella, L., Napolitano, A., & d'Ischia, M. (2003). A novel hydrogen peroxide-dependent oxidation pathway of dopamine via 6-hydroxydopamine. *Tetrahedron*, *59*(13), 2215–2221. https://doi.org/10.1016/S0040-4020(03)00242-4

Meng, X., & Fan, K. (2018). Application of nanozymes in disease diagnosis. *Progress in Biochemistry and Biophysics*, *45*(2), 218–236. https://doi.org/10.16476/j.pibb.2018.0039

Moglianetti, M., De Luca, E., Deborah, P. A., Marotta, R., Catelani, T., Sartori, B., … Pompa, P. P. (2016). Platinum nanozymes recover cellular ROS homeostasis in an oxidative stress-mediated disease model. *Nanoscale*, *8*(6), 3739–3752.

Ragg, R., Tahir, M. N., & Tremel, W. (2016). Solids Go Bio: Inorganic nanoparticles as enzyme mimics. *European Journal of Inorganic Chemistry*, *2016*(13–14), 1906–1915. https://doi.org/10.1002/ejic.201501237

Roda, A., Pasini, P., Mirasoli, M., Michelini, E., & Guardigli, M. (2004). Biotechnological applications of bioluminescence and chemiluminescence. *Trends in Biotechnology*, *22*(6), 295–303.

Santhosh, M., Chinnadayyala, S. R., Kakoti, A., & Goswami, P. (2014). Selective and sensitive detection of free bilirubin in blood serum using human serum albumin stabilized gold nanoclusters as fluorometric and colorimetric probe. *Biosensors and Bioelectronics*, *59*, 370–376. https://doi.org/10.1016/j.bios.2014.04.003

Shang, L., Dong, S., & Nienhaus, G. U. (2011). Ultra-small fluorescent metal nanoclusters: Synthesis and biological applications. *Nano Today*, *6*(4), 401–418. https://doi.org/10.1016/j.nantod.2011.06.004

Shiang, Y. C., Huang, C. C., Chen, W. Y., Chen, P. C., & Chang, H. T. (2012). Fluorescent gold and silver nanoclusters for the analysis of biopolymers and cell imaging. *Journal of Materials Chemistry*, *22*(26), 12972–12982. https://doi.org/10.1039/c2jm30563a

Silk, B. J., McCoy, M. H., Iwamoto, M., & Griffin, P. M. (2014). Foodborne Listeriosis acquired in hospitals. *Clinical Infectious Diseases*, *59*(4), 532–540.

Sivamani, E., DeLong, R. K., & Qu, R. D. (2009). Protamine-mediated DNA coating remarkably improves bombardment transformation efficiency in plant cells. *Plant Cell Reports*, *28*(2), 213–221.

Srisa-Art, M., Boehle, K. E., Geiss, B. J., & Henry, C. S. (2018). Highly sensitive detection of *Salmonella typhimurium* using a colorimetric paper-based analytical device coupled with immunomagnetic separation. *Analytical Chemistry*, *90*(1), 1035–1043.

Tao, Y., Li, M. Q., Ren, J. S., & Qu, X. G. (2015). Metal nanoclusters: Novel probes for diagnostic and therapeutic applications. *Chemical Society Reviews*, *44*(23), 8636–8663.

Tao, Y., Lin, Y., Huang, Z., Ren, J., & Qu, X. (2013). Incorporating graphene oxide and gold nanoclusters: A synergistic catalyst with surprisingly high peroxidase-like activity over a broad pH range and its application for cancer cell detection. *Advanced Materials*, *25*(18), 2594–2599. https://doi.org/10.1002/adma.201204419

Tao, Y., Lin, Y., Ren, J., & Qu, X. (2013). A dual fluorometric and colorimetric sensor for dopamine based on BSA-stabilized Au nanoclusters. *Biosensors & Bioelectronics*, *42*, 41–46. https://doi.org/10.1016/j.bios.2012.10.014

Tseng, C. W., Chang, H. Y., Chang, J. Y., & Huang, C. C. (2012). Detection of mercury ions based on mercury-induced switching of enzyme-like activity of platinum/gold nanoparticles. *Nanoscale*, *4*(21), 6823–6830.

Ueno, T., Abe, M., Hirata, K., Abe, S., Suzuki, M., Shimizu, N., … Watanabe, Y. (2009). Process of accumulation of metal ions on the interior surface of apo-ferritin: Crystal structures of a series of apo-ferritins containing variable quantities of Pd(II) ions. *Journal of the American Chemical Society*, *131*(14), 5094–5100.

Wang, G. L., Jin, L. Y., Dong, Y. M., Wu, X. M., & Li, Z. J. (2015). Intrinsic enzyme mimicking activity of gold nanoclusters upon visible light triggering and its application for colorimetric trypsin detection. *Biosensors & Bioelectronics*, *64*, 523–529. https://doi.org/10.1016/j.bios.2014.09.071

Wang, X. X., Wu, Q., Shan, Z., & Huang, Q. M. (2011). BSA-stabilized Au clusters as peroxidase mimetics for use in xanthine detection. *Biosensors & Bioelectronics*, *26*(8), 3614–3619. https://doi.org/10.1016/j.bios.2011.02.014

Wang, Y.-W., Tang, S., Yang, H.-H., & Song, H. (2016). A novel colorimetric assay for rapid detection of cysteine and Hg^{2+} based on gold clusters. *Talanta*, *146*, 71–74. https://doi.org/10.1016/j.talanta.2015.08.015

Wei, H., & Wang, E. (2013). Nanomaterials with enzyme-like characteristics (nanozymes): Next-generation artificial enzymes. *Chemical Society Reviews*, *42*(14), 6060–6093. https://doi.org/10.1039/c3cs35486e

Wennberg, R. P., Ahlfors, C. E., Bhutani, V. K., Johnson, L. H., & Shapiro, S. M. (2006). Toward understanding kernicterus: A challenge to improve the management of jaundiced newborns. *Pediatrics*, *117*(2), 474–485.

Wilcoxon, J. P., & Abrams, B. L. (2006). Synthesis, structure and properties of metal nanoclusters. *Chemical Society Reviews*, *35*(11), 1162–1194. https://doi.org/10.1039/b517312b

Wu, J., Wang, X., Wang, Q., Lou, Z., Li, S., Zhu, Y., … Wei, H. (2019). Nanomaterials with enzyme-like characteristics (nanozymes): Next-generation artificial enzymes (II). *Chemical Society Reviews*, *48*(4), 1004–1076. https://doi.org/10.1039/c8cs00457a

Xavier, P. L., Chaudhari, K., Baksi, A., & Pradeep, T. (2012). Protein-protected luminescent noble metal quantum clusters: An emerging trend in atomic cluster nanoscience. *Nanotechnology Reviews*, *3*(1), 14767. https://doi.org/10.3402/nano.v3i0.14767

Xiao, Q., Li, H. F., Hu, G. M., Wang, H. R., Li, Z. J., & Lin, J. M. (2009). Development of a rapid and sensitive magnetic chemiluminescent enzyme immunoassay for detection of luteinizing hormone in human serum. *Clinical Biochemistry*, *42*(13–14), 1461–1467.

Xie, J., Zheng, Y., & Ying, J. Y. (2009). Protein-directed synthesis of highly fluorescent gold nanoclusters. *Journal of the American Chemical Society*, *131*(3), 888–889.

Xu, S., Chen, F., Deng, M., & Sui, Y. (2014). Luminol chemiluminescence enhanced by copper nanoclusters and its analytical application. *RSC Advances*, *4*(30), 15664–15670. https://doi.org/10.1039/c4ra00516c

Xu, S., Wang, Y., Zhou, D., Kuang, M., Fang, D., Yang, W., … Ma, L. (2016). A novel chemiluminescence sensor for sensitive detection of cholesterol based on the peroxidase-like activity of copper nanoclusters. *Scientific Reports*, *6*(1), 39157. https://doi.org/10.1038/srep39157

Yamasuji, M., Shibata, T., Kabashima, T., & Kai, M. (2011). Chemiluminescence detection of telomere DNA in human cells on a membrane by using fluorescein-5-isothiocyanate-labeled primers. *Analytical Biochemistry*, *413*(1), 50–54.

Yan, Z., Niu, Q., Mou, M., Wu, Y., Liu, X., & Liao, S. (2017). A novel colorimetric method based on copper nanoclusters with intrinsic peroxidase-like for detecting xanthine in serum samples. *Journal of Nanoparticle Research*, *19*(7), 235. https://doi.org/10.1007/s11051-017-3904-9

Yang, W. T., Guo, W. S., Zhang, B. B., & Chang, J. (2014). Synthesis of noble metal nanoclusters based on protein and peptide as a template. *Acta Chimica Sinica*, *72*(12), 1209–1217. https://doi.org/10.6023/A14080568

Yang, X., & Wang, E. K. (2011). A nanoparticle autocatalytic sensor for Ag^{+} and Cu^{2+} ions in aqueous solution with high sensitivity and selectivity and its application in test paper. *Analytical Chemistry*, *83*(12), 5005–5011.

Yu, C. J., Chen, T. H., Jiang, J. Y., & Tseng, W. L. (2014). Lysozyme-directed synthesis of platinum nanoclusters as a mimic oxidase. *Nanoscale*, *6* (16), 9618–9624. https://doi.org/10.1039/c3nr06896j

Yu, Y., Mok, B. Y. L., Loh, X. J., & Tan, Y. N. (2016). Rational design of biomolecular templates for synthesizing multifunctional noble metal nanoclusters toward personalized theranostic applications. *Advanced Healthcare Materials*, *5*(15), 1844–1859. https://doi.org/10.1002/adhm.201600192

Zhu, R., Zhou, Y., Wang, X.-L., Liang, L.-P., Long, Y.-J., Wang, Q.-L., … Zheng, H.-Z. (2013). Detection of Hg^{2+} based on the selective inhibition of peroxidase mimetic activity of BSA-Au clusters. *Talanta*, *117*, 127–132. https://doi.org/10.1016/j.talanta.2013.08.053

How to cite this article: Meng X, Zare I, Yan X, Fan K. Protein-protected metal nanoclusters: An emerging ultra-small nanozyme. *WIREs Nanomed Nanobiotechnol*. 2019;e1602. https://doi.org/10.1002/wnan.1602